Journal of Scientific Computing (2022) 93:12
https://doi.org/10.1007/s10915-022-01949-x

Immersed Virtual Element Methods for Elliptic Interface Problems in Two Dimensions

Shuhao Cao[1] · **Long Chen**[2] · **Ruchi Guo**[2] · **Frank Lin**[2]

Received: 8 December 2021 / Revised: 29 June 2022 / Accepted: 29 June 2022 /
Published online: 22 August 2022
© The Author(s), under exclusive licence to Springer Science+Business Media, LLC, part of Springer Nature 2022

Abstract
This article presents an immersed virtual element method for solving a class of interface problems that combines the advantages of both body-fitted mesh methods and unfitted mesh methods. A background body-fitted mesh is generated initially. On those interface elements, virtual element spaces are constructed as solution spaces to local interface problems, and exact sequences can be established for these new spaces involving discontinuous coefficients. The discontinuous coefficients of interface problems are recast as Hodge star operators that are the key to project immersed virtual functions to classic immersed finite element (IFE) functions for computing numerical solutions. An a priori convergence analysis is established robust with respect to the interface location. The proposed method is capable of handling more complicated interface element configuration and provides better performance than the conventional penalty-type IFE method for the $\mathbf{H}$(curl)-interface problem arising from Maxwell equations. It also brings a connection between various methods such as body-fitted methods, IFE methods, virtual element methods, etc.

Keywords H^1 and $\mathbf{H}$(curl) Interface problems · Fitted mesh methods · Unfitted mesh methods · Virtual element methods · Immersed finite element methods · de Rham complex

Mathematics Subject Classification 65N15 · 65N30

This work was funded in part by NSF grants DMS-1913080 and DMS-2012465.

✉ Ruchi Guo
ruchig@uci.edu

Shuhao Cao
sch59@umkc.edu

Long Chen
chenlong@math.uci.edu

Frank Lin
fmlin@uci.edu

[1] Division of Computing, Analytics, and Mathematics, School of Science and Engineering, University of Missouri Kansas City, Kansas City, MO, United States

[2] Department of Mathematics, University of California Irvine, Irvine, CA, United States

1 Introduction

Interface problems widely appear in many engineering and physical applications involving multiple materials or media that incorporate discontinuous coefficients for the related partial differential equations (PDEs). For example, Fig. 1 illustrates a two-dimensional bounded domain Ω that is formed by two different materials separated by a closed smooth curve $\Gamma \in C^{1,1}$, i.e., Γ separates Ω into subdomains Ω^+ and Ω^- such that $\overline{\Omega} = \overline{\Omega^+ \cup \Omega^- \cup \Gamma}$. The main challenge of using standard finite element methods (FEMs) is that solutions of interface problems are not smooth across the interface. It is well known that FEMs can be used to solve interface problems with optimal accuracy [21, 49, 55, 74, 76] based on body-fitted and shape regular meshes. The "body-fittedness" refers to that the interface is well approximated by edges of elements [49], i.e., the piecewise linear approximated interface cannot intersect any element interior. However, it is nontrivial and time-consuming to generate such a shape regular mesh that fits the interface, as it generally requires certain global modifications. This issue will become more severe for complex geometry or moving interface problems, especially in three dimensions.

So, it becomes critical for the purpose of efficiency to relax the mesh restriction for interface problems. Generally speaking, two different groups of methods can be found in this field: (i) modify the finite element spaces or finite difference stencils to encode the jump conditions into the discretization; (ii) modify the mesh only near the interface and then apply either continuous or discontinuous Galerkin formulation.

The first approach employs meshes that are completely independent of the interface, i.e., the so-called unfitted mesh methods. As the mesh cannot resolve interface geometry, special treatments are needed on interface elements. The Nitsche's idea [60] uses penalties to enforce the jump condition, see e.g., CutFEM [9] or unfitted FEM [33]. Another strategy is to construct special FEM functions or finite difference stencils on interface elements, such as the immersed interface method [48], the MIB method [75], the multiscale FEM [23], and the immersed finite element (IFE) methods [32, 52, 53] to be discussed. In particular, for the IFE method, a set of local basis functions on interface elements are devised as piecewise polynomials that include jump conditions in their connection in a pointwise or an averaging sense. The convergence of IFE methods for H^1 interface problems have been established in [32, 52, 53] and improved recently in [28, 30, 43, 44]. These methods still obtain the

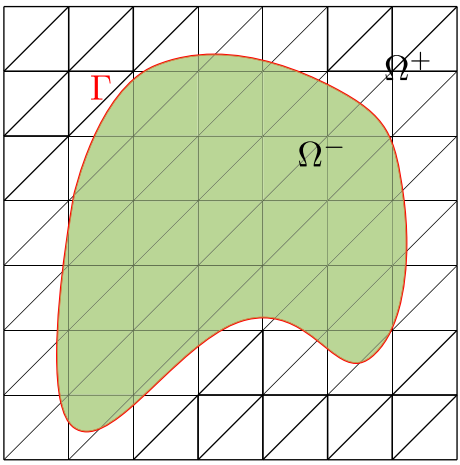

Fig. 1 The domain and a uniform triangulation for the interface problem

optimal convergence order where the hidden constant is independent of the interface location relative to the mesh. However, for almost all these unfitted mesh methods, the approximation spaces are not conforming. The non-conformity actually becomes an essential issue for solving $\mathbf{H}(\text{curl})$ interface problems arising from Maxwell equations, which has been widely discussed in the literature [7, 14, 15, 31, 38], also see the discussion below. It is one of the motivation for the proposed method that aims to develop a method based on conforming approximation spaces.

For the second approach, as the modification is only performed locally near the interface, shape regularity, in general, cannot be achieved. Instead, the refined meshes are required to satisfy the maximum angle condition [4, 46, 47] to obtain optimal convergence rates robust with respect to element shapes. One work in this direction can be found in [20]. This is indeed achievable for the 2D case, as the maximum angle condition can be always satisfied for arbitrary interface location [12], and even for adaptive meshes [72]. However, such a local triangulation satisfying the maximum angle condition might not be readily available or requires strenuous effort to generate in the 3D case [26, 50, 57]. This obstacle also motivates us to develop a method that does not rely on a local triangulation. Even though the current work is only for the 2D problems, it can shed light on the 3D case. In fact, we have recently established the 3D IVE spaces in [13] after this work.

Recently, the authors in [18] proposed a novel method that directly works on polygonal or polyhedral elements cut from interface, instead of re-triangulating them to simplices. The key of [18] is to employ directly the virtual element method (VEM) on these elements for the discretization, on which only degrees of freedom (DoFs) are necessary for assembling the final linear system, e.g., see [63, 65, 66, 70] and the reference therein. The "virtual" shape functions, which are H^1 functions that serve as the solutions to certain local problems but do not need to be explicitly solved, are then projected to polynomial spaces for computation through DoFs. One key advantage is its flexibility for element shapes being polygonal or polyhedral. As the interface may intersect elements arbitrarily which generates elements with high aspect ratio, for the aforementioned approach in [18], one major difficulty is to obtain a robust a priori error estimate independent of the potentially anisotropic subelement shapes. Some anisotropic error analysis of VEM can be found in [10–12] for different interface problems.

Inspired by VEM [18] and IFE methods in the literature, is it possible for a numerical method to take both the advantages of conformity provided by virtual element spaces and robust optimal approximation capabilities of IFE spaces? The question severs as one major motivation for this work. For this purpose, we shall develop H^1, $\mathbf{H}(\text{curl})$ and $\mathbf{H}(\text{div})$ virtual element spaces involving discontinuous coefficients, i.e., they are solution spaces to some local interface problems incorporating jump conditions related to the underlying equations. As the interface is immersed into the design of the virtual element spaces, we shall call it *immersed (interface) virtual element method* (IVEM). The key idea is to use the conforming virtual element spaces on a shape regular background unfitted mesh $\mathcal{T}_h$ for discretization, and then to project them to the IFE spaces on interface elements which are cut by the interfaces from the background mesh. The virtual element space provides the conformity and the IFE space can offer sufficient and robust approximation capabilities locally. We also note that this practice exhibits similarity to the Trefftz finite element method (Trefftz-FEM) [45], in which the basis functions are fundamental solutions to certain local problems. Another resemblance is that Trefftz FEM may relax the exact inter-element continuity to yield a "quasi-conforming" discretization [2, 41], which carries the same spirit with the IFE spaces locally. Moreover, as subelements of elements are treated together through the jump conditions instead of independently as anisotropic polygons, it is highlighted that the coercivity can

be established of which the hidden constants are independent of subelement shapes. This property does not hold for virtual element spaces defined only on subelements [10, 18], where the coercivity constant may depend on the anisotropy of polygons or polyhedra, and refined analysis is needed to establish a robust error analysis.

In particular, we will consider the following H^1 and $\mathbf{H}(\mathrm{curl})$ interface problems in two dimensions and refer to [42] for $\mathbf{H}(\mathrm{div})$ interface problems. Due to the fact that solution exhibiting low regularity near the interface, especially for the $\mathbf{H}(\mathrm{curl})$ equations [24, 25], in this work we only consider the lowest order methods. The first problem of interest is an H^1-elliptic interface problem

$$\begin{aligned} -\nabla\cdot(\beta\nabla u) &= f \quad \text{in } \Omega^-\cup\Omega^+,\\ u &= 0 \quad \text{on } \partial\Omega, \end{aligned} \tag{1.1}$$

with $f\in L^2(\Omega)$, and the continuity and flux jump conditions

$$[u]_\Gamma := u^+ - u^- = 0, \tag{1.2a}$$

$$[\beta\nabla u\cdot\mathbf{n}]_\Gamma := \beta^+\nabla u^+\cdot\mathbf{n} - \beta^-\nabla u^-\cdot\mathbf{n} = 0, \tag{1.2b}$$

where $\mathbf{n} := \mathbf{n}(\mathbf{x})$ denotes the unit normal vector to Γ at $\mathbf{x} = (x_1, x_2)\in\Gamma$ pointing from Ω^- to Ω^+. In the following discussion, $\mathbf{n}$ always denotes the unit outward normal vector, and $\mathbf{t}$ denotes the tangential vector which is a counterclockwise rotation of $\mathbf{n}$ by $\pi/2$.

The second model we are interested in is an $\mathbf{H}(\mathrm{curl})$ interface problem arising from Maxwell equations:

$$\mathbf{curl}\,(\alpha\,\mathrm{curl}\,\mathbf{u}) + \beta\mathbf{u} = \mathbf{f} \qquad \text{in } \Omega^-\cup\Omega^+, \tag{1.3a}$$

$$\mathbf{u}\cdot\mathbf{t} = 0 \qquad \text{on } \partial\Omega, \tag{1.3b}$$

with $\mathbf{f}\in\mathbf{H}(\mathrm{div};\Omega)$, where the operator curl is for vector functions $\mathbf{v} = (v_1, v_2)^\intercal$ such that $\mathrm{curl}\,\mathbf{v} = \partial_{x_1}v_2 - \partial_{x_2}v_1$ while $\mathbf{curl}$ is for scalar functions v such that $\mathbf{curl}\,v = \left(\partial_{x_2}v, -\partial_{x_1}v\right)^\intercal$ with "$\intercal$" denoting the transpose herein. The following jump conditions at the interface Γ are imposed:

$$[\mathbf{u}\cdot\mathbf{t}]_\Gamma := \mathbf{u}^+\cdot\mathbf{t} - \mathbf{u}^-\cdot\mathbf{t} = 0, \tag{1.4a}$$

$$[\alpha\,\mathrm{curl}\,\mathbf{u}]_\Gamma := \alpha^+\mathrm{curl}\,\mathbf{u}^+ - \alpha^-\mathrm{curl}\,\mathbf{u}^- = 0, \tag{1.4b}$$

$$[\beta\mathbf{u}\cdot\mathbf{n}]_\Gamma := \beta^+\mathbf{u}^+\cdot\mathbf{n} - \beta^-\mathbf{u}^-\cdot\mathbf{n} = 0. \tag{1.4c}$$

In Eqs. (1.1) and (1.3), the coefficients α and β in Ω are assumed to be positive piecewise constant functions of which the locations of the discontinuity align with one another:

$$\alpha(x,y) = \begin{cases}\alpha^+, & (x,y)\in\Omega^+,\\ \alpha^-, & (x,y)\in\Omega^-,\end{cases} \qquad \beta(x,y) = \begin{cases}\beta^+, & (x,y)\in\Omega^+,\\ \beta^-, & (x,y)\in\Omega^-.\end{cases}$$

Note that the two models above share the same parameter β which can be interpreted from the perspective of de Rham complexes. The proposed virtual element spaces can inherit this kind of structure on each interface element.

Similar to the standard virtual element spaces in the literature, our new H^1, $\mathbf{H}(\mathrm{curl})$ and $\mathbf{H}(\mathrm{div})$ virtual element spaces admit the nodal and edge DoFs which make them conforming in their respective Sobolev spaces even with the presence of interface-cutted mesh and discontinuous parameters. These DoFs also enable us to establish the global exact sequence, and e.g., the following commutative diagrams

$$\begin{array}{ccccccccc} \mathbb{R} & \longrightarrow & H^2(\beta;\mathcal{T}_h) & \xrightarrow{\nabla} & \mathbf{H}^1(\mathrm{curl},\alpha,\beta;\mathcal{T}_h) & \xrightarrow{\mathrm{curl}} & H^1(\alpha;\mathcal{T}_h) & \longrightarrow & 0 \\ & & \downarrow I_h^n & & \downarrow I_h^e & & \downarrow \pi_h^{\alpha_h} & & \\ \mathbb{R} & \longrightarrow & V_h^n & \xrightarrow{\nabla} & \mathbf{V}_h^e & \xrightarrow{\mathrm{curl}} & Q_h^{\alpha_h} & \longrightarrow & 0. \end{array} \tag{1.5}$$

See Sects. 2.2 and 3.1 for definitions of spaces and operators.

Constructing special shape functions by solving local problems to capture certain behavior of solutions can be traced back to the fundamental work of Babuška et al. in [5, 6]. In particular, for a 1D case, the basis functions in [5, 6] are the solutions of

$$-(\beta(x)u')' = 0 \qquad \text{in } [a,b] \tag{1.6}$$

subject to some boundary conditions at the ending points a, b. It could be considered as the local problems of VEM with variable coefficients. Due to the trivial 1D geometry, solutions of (1.6) can be expressed as $\int_a^x \beta^{-1}(s)\,\mathrm{d}s$. When β is a piecewise constant function, they become exactly the 1D IFE functions [51]. Namely, for this case, the 1D VEM and IFE spaces are identical, but they are distinguished in higher dimensions due to more complicated geometry. From this point of view, on one hand, the proposed IVEM is a more straightforward generalization of the early approach of Babuška et al. On the other hand, the conventional IFE space is also important to provide robust local approximation capabilities, and thus is suitable for constructing projections.

We also note that the newly constructed H^1 virtual element space is similar to the multiscale finite element space in [23] in the sense that local interface problems are used to develop the approximation spaces. In both approaches, standard non-piecewise polynomials on interface elements cannot be used to approximate the solutions to these local interface problems due to the jump conditions across the interface. In [23], the authors generate a local fine mesh and use standard finite element functions for approximation. Here we propose projecting the virtual element spaces to IFE spaces consisting of piecewise polynomials that can accurately capture the jump conditions. We will show that, similar to the conventional VEM, these projections are indeed computable directly through the DoFs.

The proposed method is not only a new formulation of IFE or VEM in the literature, but also inherits the advantages of both the two methods, or even the general fitted mesh and unfitted mesh methodology. First, it is still able to solve interface problems on a background unfitted mesh. However, different from most of the unfitted mesh methods aforementioned that do not impose any DoFs on edges or nodes associated with cutting points of interface, the proposed one does impose these newly added DoFs. With this property, it may better resolve the more complex geometry but without generating an extra triangulation near the interface. In other words, we use a virtual body-fitted mesh. Second, it is known that IFE shape functions satisfying certain DoFs are in general not easy to construct, and theoretically their existence are subject to some geometric conditions [28, 31, 42]. Within the VEM framework, this issue has been completely addressed, since the DoFs are imposed through virtual functions which always exist by solving local problems. Third, compared with the anisotropic analysis for conventional VEM [8, 10], the robust error analysis of the proposed method can be, thanks to the shape regularity of background meshes and properties of IFE spaces, easily and systematically obtained regardless of subelement shape. Finally, compared with other penalty-type methods in the literature [30, 53], the proposed method requires only a locally computed edge term within each element, and thus makes the assembling procedure easier as the stabilization term does not need explicitly the interaction of neighbor elements' DoFs.

One remarkable advantage of using the proposed method is to recover the optimal convergence for solving $\mathbf{H}(\mathrm{curl})$ interface problems on unfitted meshes. The $\mathbf{H}(\mathrm{curl})$ equations

are sensitive to the conformity of the approximated spaces due to its low regularity. Discontinuous Galerkin methods can obtain an optimal convergence, but this is based on the fact that the broken non-conforming space contains an $\mathbf{H}(\mathrm{curl})$-conforming subspace when no interface is present, see the analysis in [35–37]. Unfortunately, many aforementioned conventional unfitted mesh methods do not preserve this property which may cause the loss of accuracy. This phenomenon has been numerically observed and theoretically proved in [14, 15] for Nitsche's penalty methods. In [54], the authors assume a higher regularity, i.e., at least piecewise $H^2(\Omega^{\pm})$, to overcome this issue. As for IFE methods, standard penalty-type methods still do not achieve optimal convergence, and a Petrov-Galerkin method can be applied, see [31], and achieve optimal order convergence with certain conditions. The IVEM proposed in this paper is able to circumvent this issue since the underlying IVE space is always conforming which is distinguished from many conventional unfitted mesh methods. The resulting linear algebraic system remains symmetric and positive definite unlike the one obtained from Petrov-Galerkin formulation [31]. Again due to the usual low piecewise $\mathbf{H}^1(\mathrm{curl})$ regularity near the interface for the $\mathbf{H}(\mathrm{curl})$ equations, in this work we only consider the lowest order methods.

The rest of this article is organized as follows. In Sect. 2, some existing results are presented to help us to establish the error analysis. In Sect. 3, we introduce the IVE space and its properties, and review IFE spaces. In Sect. 4, we show some novel estimates for IFE spaces that help in our error analysis. In Sect. 5 and Sect. 6, the convergence is shown for the H^1 and $\mathbf{H}(\mathrm{curl})$ interface problems, respectively.

2 Preliminary

In this section, we introduce some mesh assumptions and define some notation. We also recall some existing fundamental estimates which are critical for our analysis. Throughout this paper, we assume $\Omega \subset \mathbb{R}^2$ is a simply connected convex polygon. Usually it can be chosen as a rectangle enclosing the interface.

2.1 Meshes

Let $\mathcal{T}_h = \{K\}$ be a shape regular triangulation of the domain Ω that may not be fitted to the interface. A triangle K is called an interface triangle if $|K \cap \Omega^+| > 0$ and $|K \cap \Omega^-| > 0$; otherwise K is called a non-interface element. The collection of interface elements and non-interface elements are denoted as $\mathcal{T}_h^i$ and $\mathcal{T}_h^n$, respectively.

For a non-interface element K, the local finite element space is simply defined as the linear polynomial space $\mathbb{P}_1(K)$ for (1.1) or the lowest order Nédélec space $\mathcal{ND}_0(K)$ [56, 58] for (1.3a). The usage whether to choose the nodal or edge shape functions depends on the problem. For convenience of the reader, $\mathcal{RT}_0(K)$ is the lowest order Raviart-Thomas space [61] on K as well. If $K \in \mathcal{T}_h^i$, see Fig. 2a for example, $\mathbf{b}_1$ and $\mathbf{b}_2$ denote the intersection points of the interface and ∂K, and we let $\Gamma_h^K = \mathbf{b}_1\mathbf{b}_2$. In addition, we let $\mathcal{N}_K$ be collection of vertices and cutting points of K, and let $\mathcal{E}_K$ be collection of cut segments from the original edges of K, for example $\mathcal{N}_K = \{\mathbf{a}_1, \mathbf{a}_2, \mathbf{a}_3, \mathbf{b}_1, \mathbf{b}_2\}$ and $\mathcal{E}_K = \{\mathbf{a}_1\mathbf{b}_1, \mathbf{b}_1\mathbf{a}_2, \mathbf{a}_2\mathbf{a}_3, \mathbf{a}_3\mathbf{b}_2, \mathbf{b}_2\mathbf{a}_1\}$ for the interface element K in Fig. 2a. Namely, we treat K as pentagon instead of a triangle. Moreover, let $\mathcal{N}_h$ and $\mathcal{E}_h$ be the collection of all the vertices and edges of $\mathcal{N}_K$ and $\mathcal{E}_K$ overall all the K, respectively. Although the conventional IFE methods may be only used on the

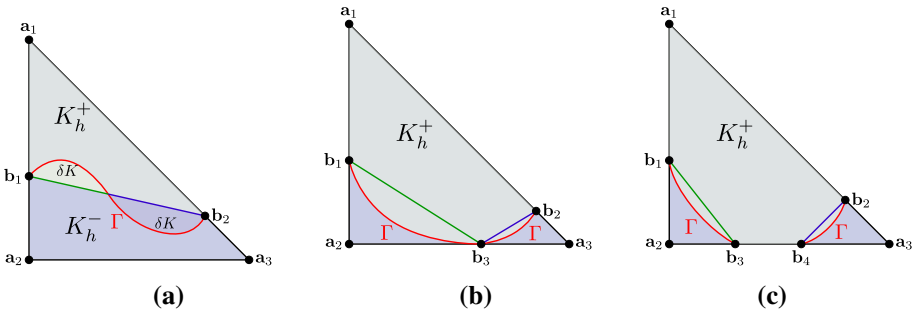

Fig. 2 Possible configuration for an interface element. **a**, **b**, **c**: Γ intersects at an interface at 2, 3, 4 points. The proposed IVE spaces can be defined on almost arbitrary interface element configuration, as discussed in Sect. 3.1. But the construction of IFE spaces and the error analysis will be a little more technical for those general cases. So for simplicity, we will only consider the case in (2a) for the discussion starting from Sect. 3.2

element in Fig. 2a that has two cutting point on two different edges, the proposed method can be readily used for elements with more complex geometry such as those in Figs. 2b and c.

We define the union of cut segments Γ_h^K of all the interface elements as the approximated interface Γ_h, which also separates the original domain Ω into two subdomains $\Omega_h^{\pm}$, in which the $\pm$ are determined by the area overlap with $\Omega^{\pm}$. Define $\alpha_h = \alpha^{\pm}$, $\beta_h = \beta^{\pm}$ on $\Omega_h^{\pm}$. For each interface triangle K, δK is the subset of K such that $\beta \neq \beta_h$ (i.e. mismatch region). Using Fig. 2a as an example, without loss of generality, $K_h^+ := \text{int Conv}(\mathbf{a}_1\mathbf{b}_1\mathbf{b}_2)$ and K_h^- is the quadrilateral complement formed by $\text{int Conv}(\mathbf{a}_2\mathbf{a}_3\mathbf{b}_2\mathbf{b}_1)$, where int stands for the interior so that $K_h^{\pm}$ are open sets, and the relevant definitions and proofs follow similarly when $\pm$ swaps.

2.2 Sobolev Spaces and Norms

Let $H^k(D)$ ($k \geq 0$) be the standard Sobolev space on a domain D with the norm $\|\cdot\|_{H^k(D)}$, as well as the seminorm $|\cdot|_{H^k(D)}$ when $k > 0$. Due to the discontinuity of the coefficient β, the solution to the H^1 interface problem in (1.1) is not in $H^2(\Omega)$ globally. To define this piecewise Sobolev space, for any open subdomain $D \subset \Omega$ intersecting Γ, $D^{\pm} := D \cap \Omega^{\pm}$, we introduce

$$H^k(\cup D^{\pm}) = \left\{u \in H^1(D) \text{ and } u^{\pm} \in H^k(D^{\pm})\right\}$$

and the piecewise H^k–norm is defined by $\|u\|^2_{H^k(\cup D^{\pm})} = \|u\|^2_{H^k(D^+)} + \|u\|^2_{H^k(D^-)}$ for any $u \in H^k(\cup D^{\pm})$. If there is no danger of confusion, in the following discussion, we shall employ a simple notation for the norms: $\|\cdot\|_{k,D} = \|\cdot\|_{H^k(D)}$ and $\|\cdot\|_{k,\cup D^{\pm}} = \|\cdot\|_{H^k(\cup D^{\pm})}$, and the seminorms follow similarly. For the $\mathbf{H}(\text{curl})$ interface problem, we let

$$\mathbf{H}^k(\text{curl}; D) = \{\mathbf{u} \in \mathbf{H}(\text{curl}; D) : \text{curl } \mathbf{u} \in \mathbf{H}^k(D)\},$$
$$\mathbf{H}^k(\text{div}; D) = \{\mathbf{u} \in \mathbf{H}(\text{div}; D) : \text{div } \mathbf{u} \in H^k(D)\}.$$

In addition, we introduce the following spaces

$$H^2(\beta; \mathcal{T}_h) = H^1(\Omega) \cap \{u : u|_K \in H^2(K),\ \forall K \in \mathcal{T}_h^n\} \cap \{u : u|_K \in H^2(\cup K^{\pm}),\ \beta\nabla u|_K \in \mathbf{H}(\text{div}; K),\ \forall K \in \mathcal{T}_h^i\}, \quad (2.1a)$$

$$\mathbf{H}^1(\mathrm{curl}, \alpha, \beta; \mathcal{T}_h) = \mathbf{H}(\mathrm{curl}; \Omega) \cap \{\mathbf{u} : \mathbf{u}|_K \in \mathbf{H}^1(\mathrm{curl}; K),\ \forall K \in \mathcal{T}_h^n\} \cap \{\mathbf{u} : \mathbf{u}|_K \in \mathbf{H}^1(\mathrm{curl}; \cup K^{\pm}),\ \beta\mathbf{u}|_K \in \mathbf{H}(\mathrm{div}; K), \alpha\,\mathrm{curl}\,\mathbf{u}|_K \in H^1(K),\ \forall K \in \mathcal{T}_h^i\}, \tag{2.1b}$$

$$\mathbf{H}^1(\mathrm{div}, \beta; \mathcal{T}_h) = \mathbf{H}(\mathrm{div}; \Omega) \cap \{\mathbf{u} : \mathbf{u}|_K \in \mathbf{H}^1(\mathrm{div}; K),\ \forall K \in \mathcal{T}_h^n\} \cap \{\mathbf{u} : \mathbf{u}|_K \in \mathbf{H}^1(\mathrm{div}; \cup K^{\pm}),\ \beta\mathbf{u}|_K \in \mathbf{H}(\mathrm{curl}; K),\ \forall K \in \mathcal{T}_h^i\}, \tag{2.1c}$$

$$H^1(\alpha; \mathcal{T}_h) = L^2(\Omega) \cap \{u : u|_K \in H^1(K),\ \forall K \in \mathcal{T}_h^n\} \cap \{u : u|_K \in H^1(\cup K^{\pm}),\ \alpha u|_K \in H^1(K),\ \forall K \in \mathcal{T}_h^i\}. \tag{2.1d}$$

It is not hard to see these spaces are mesh-dependent and are constructed based on the associated jump conditions. Under the setting introduced in Sect. 1 that $f \in L^2(\Omega)$ and $\Gamma \in C^{1,1}$, it can be shown that (see e.g. [22, 23, 39]), the solution to the H^1 elliptic interface problem satisfies $u \in H^2(\cup\Omega^{\pm})$, and thus, with the jump conditions, $u \in H^2(\beta; \mathcal{T}_h)$. As for the $\mathbf{H}(\mathrm{curl})$ interface problem, we follow [34, 40] to assume $\mathbf{u} \in \mathbf{H}^1(\mathrm{curl}; \cup\Omega^{\pm})$. With the jump condition, we have $\mathbf{u} \in \mathbf{H}^1(\mathrm{curl}, \alpha, \beta; \mathcal{T}_h)$.

Given an interface element K, we let $H^2(\beta; K)$, $\mathbf{H}^1(\mathrm{curl}, \alpha, \beta; K)$ and $H^1(\alpha; K)$ be the local spaces on K of their respective global counterpart in (2.1), with the inter-element continuity constraint removed. These spaces together with the classic Sobolev spaces admit the following diagram in the continuous level:

$$\begin{array}{ccccccccc} \mathbb{R} & \longrightarrow & H^2(\beta; K) & \xrightarrow{\nabla} & \mathbf{H}^1(\mathrm{curl}, \alpha, \beta; K) & \xrightarrow{\mathrm{curl}} & H^1(\alpha; K) & \longrightarrow & 0 \\ & & \downarrow I & & \downarrow \beta & & \downarrow \alpha & & \\ 0 & \longleftarrow & L^2(K) & \xleftarrow{\mathrm{div}} & \mathbf{H}(\mathrm{div}; K) & \xleftarrow{\mathbf{curl}} & H^1(K) & \longleftarrow & \mathbb{R}. \end{array} \tag{2.2}$$

We highlight that the scalar multiplication $\beta\cdot$ and $\alpha\cdot$ can be understood as Hodge stars [3] as shown by the downward arrows in (2.2). We shall construct virtual element spaces to mimic this diagram in the discrete level.

Lemma 1 *Assume that Γ is C^2 smooth and $\partial\Omega$ is a polygon, $\Gamma \cap \partial\Omega = \varnothing$. Then,*

$$\mathbb{R} \longrightarrow H^2(\beta; \mathcal{T}_h) \xrightarrow{\nabla} \mathbf{H}^1(\mathrm{curl}, \alpha, \beta; \mathcal{T}_h) \xrightarrow{\mathrm{curl}} H^1(\alpha; \mathcal{T}_h) \longrightarrow 0 \tag{2.3}$$

is exact.

Proof We first recall the standard exact sequence of the de Rham complex:

$$\mathbb{R} \longrightarrow H^1(D) \xrightarrow{\nabla} \mathbf{H}(\mathrm{curl}; D) \xrightarrow{\mathrm{curl}} L^2(D) \longrightarrow 0, \tag{2.4}$$

where D is any contractible subdomain of Ω with Lipschitz boundary ∂D.

By definition, for $v \in H^2(\beta; \mathcal{T}_h)$, $\nabla v \in \mathbf{H}(\mathrm{curl}; \Omega)$ satisfies the regularity condition and the jump conditions associated with $\mathbf{H}^1(\mathrm{curl}, \alpha, \beta; \mathcal{T}_h)$ and obviously $\mathrm{curl}\,\nabla v = 0$. Conversely, let $\mathbf{u} \in \mathbf{H}^1(\mathrm{curl}, \alpha, \beta; \mathcal{T}_h)$ such that $\mathrm{curl}\,\mathbf{u} = 0$. We are going to find $v \in H^2(\beta; \mathcal{T}_h)$ such that $\mathbf{u} = \nabla v$. By the standard exact sequence, there exists $v \in H^1(\Omega)$ such that $\nabla v = \mathbf{u}$. We need to verify the extra conditions associated with $H^2(\beta; \mathcal{T}_h)$ for v. Given each $K \in \mathcal{T}_h^n$, $\nabla v = \mathbf{u} \in \mathbf{H}^1(K)$ implies $v \in H^2(K)$. On each $K \in \mathcal{T}_h^i$, similarly $\nabla v = \mathbf{u} \in \mathbf{H}^1(\cup K^{\pm})$ implies $v \in H^2(\cup K^{\pm})$. In addition, $\beta\nabla v \in \mathbf{H}(\mathrm{div}; K)$ is trivial by (2.1b). Thus, $v \in H^2(\beta; \mathcal{T}_h)$.

Next, let us show $\mathrm{curl} : \mathbf{H}^1(\mathrm{curl}, \alpha, \beta; \mathcal{T}_h) \to H^1(\alpha; \mathcal{T}_h)$ is surjective. Since Ω may not be convex, we let $\widetilde{\Omega}$ be convex hull of Ω. For any $f \in H^1(\alpha; \mathcal{T}_h) \subset L^2(\Omega)$, we let $\tilde{f}$ be

the trivial zero extension of f to $\widetilde{\Omega}$, and thus $\tilde{f} \in L^2(\widetilde{\Omega})$. Since Γ does not intersect $\partial\Omega$, it can also partition $\widetilde{\Omega}$ into interior and exterior subdomains denoted by $\widetilde{\Omega}^{\pm}$. Then, β^+ can be naturally used on $\widetilde{\Omega}^+$. Thus, without loss of generality, we shall keep the same notation. Consider a function φ such that

$$\begin{aligned} \operatorname{curl} \beta^{-1}\mathbf{curl}\,\varphi = -\operatorname{div}(\beta^{-1}\nabla\varphi) = \tilde{f} \quad & \text{in } \cup\,\widetilde{\Omega}^{\pm}, && (2.5a)\\ [\varphi]_{\Gamma} = 0, \quad & \text{on } \Gamma, && (2.5b)\\ [\beta^{-1}\nabla\varphi\cdot\mathbf{n}]_{\Gamma} = 0, \quad & \text{on } \Gamma, && (2.5c)\\ \beta^{-1}\nabla\varphi\cdot\mathbf{n} = |\partial\widetilde{\Omega}|^{-1}\int_{\Omega}\tilde{f}\,\mathrm{d}\mathbf{x} \quad & \text{on } \partial\widetilde{\Omega}. && (2.5d) \end{aligned}$$

Note that (2.5) is a pure Neumann boundary value problem with the compatibility satisfied, which guarantees the solution φ being unique up to a constant. Thus, $\mathbf{curl}\,\varphi$ is unique and we let $\tilde{\mathbf{w}} = \beta^{-1}\mathbf{curl}\,\varphi$. As $\tilde{f} \in L^2(\widetilde{\Omega})$ with $\widetilde{\Omega}$ being convex and Γ being C^2 smooth, by the elliptic regularity we have $\varphi \in H^2(\cup\widetilde{\Omega}^{\pm})$ [39], thus further obtain $\tilde{\mathbf{w}}|_{\widetilde{\Omega}^{\pm}} \in \mathbf{H}^1(\widetilde{\Omega}^{\pm})$. Besides, (2.5a) shows $\operatorname{curl}\tilde{\mathbf{w}} = \tilde{f}$ in $\widetilde{\Omega}^{\pm}$, (2.5b) shows $[\beta\tilde{\mathbf{w}}\cdot\mathbf{n}]_{\Gamma} = [\mathbf{curl}\,\varphi\cdot\mathbf{n}]_{\Gamma} = [\nabla\varphi\cdot\mathbf{t}]_{\Gamma} = 0$, and (2.5c) yields $[\tilde{\mathbf{w}}\cdot\mathbf{t}]_{\Gamma} = [\beta^{-1}\mathbf{curl}\,\varphi\cdot\mathbf{t}]_{\Gamma} = [\beta^{-1}\nabla\varphi\cdot\mathbf{n}]_{\Gamma} = 0$. Therefore, $\mathbf{w} := \tilde{\mathbf{w}}|_{\Omega} \in \mathbf{H}^1(\operatorname{curl},\alpha,\beta;\mathcal{T}_h)$ which completes the proof. □

Remark 1 Lemma 1 heavily relies on the smoothness of Γ due to the interface problem (2.5). If the interface is non-smooth or touches the boundary $\partial\Omega$, the solution regularity, in general, will not be as high as $\mathbf{H}^1(\operatorname{curl})$.

Next, $u_E^{\pm} := Eu^{\pm} \in H^2(\Omega)$ denotes the standard smooth Sobolev extensions that are bounded in the H^2-norm (see e.g., [1]). As for the $\mathbf{H}(\operatorname{curl})$ spaces, the continuous extension operator is given by the following result:

Theorem 2.1 (Theorem 3.4 and Corollary 3.5 in [34]) *There exist two bounded linear operators*

$$\mathbf{E}^{\pm}_{\operatorname{curl}} : \mathbf{H}^1(\operatorname{curl};\Omega^{\pm}) \to \mathbf{H}^1(\operatorname{curl};\Omega) \tag{2.6}$$

such that for each $\mathbf{u} \in \mathbf{H}^1(\operatorname{curl};\Omega^{\pm})$*:*

1. $\mathbf{E}^{\pm}_{\operatorname{curl}}\mathbf{u} = \mathbf{u}$ *a.e. in* $\Omega^{\pm}$.
2. $\|\mathbf{E}^{\pm}_{\operatorname{curl}}\mathbf{u}\|_{\mathbf{H}^1(\operatorname{curl};\Omega)} \le C_E\|\mathbf{u}\|_{\mathbf{H}^1(\operatorname{curl};\Omega^{\pm})}$ *with constant* C_E *only depending on* Ω *and* Γ.

Using the extension operators, we can define $\mathbf{u}_E^{\pm} = \mathbf{E}^{\pm}_{\operatorname{curl}}\mathbf{u}^{\pm}$ which are the keys in the analysis later.

In the rest of the paper, all constants in $\lesssim$ are β and α–dependent but independent of the cut point locations unless stated otherwise.

2.3 Fundamental Inequalities

We review some fundamental estimates that are crucial for our analysis. The first one concerns the mismatch region of the partitions by the exact interface Γ and Γ_h^K, i.e., δK. For any subdomain $D \subseteq \Omega$ with the interface Γ, define

$$D_{\delta} = \{x \in D : \operatorname{dist}(x,\Gamma) < \delta\}.$$

Clearly, there hold

$$\bigcup_{K\in\mathcal{T}_h^i}\delta K \subset \Omega_{\delta_0}, \qquad \text{and} \qquad \bigcup_{K\in\mathcal{T}_h^i} K \subset \Omega_{h_\Gamma}$$

where δ_0 is the maximum distance from Γ_h to Γ, while h_Γ is the maximum diameter of $K \in \mathcal{T}_h^i$ with $h_\Gamma \lesssim h$. By well-known geometric estimates, e.g., see [28, Lemma 3.2], we have $\delta_0 \lesssim h^2$. The following result can be found in [19, 49].

Lemma 2 (A norm estimate on a strip region) *For each $u \in H^1(\cup \Omega^\pm)$, there holds*

$$\|u\|_{0,\Omega_\delta} \lesssim \sqrt{\delta}\|u\|_{1,\cup\Omega^\pm}.$$

We will also need the following trace theorems and Poincaré-type inequalities.

Lemma 3 (A trace inequality [8]) *Let e be an edge of a shape regular element K. Then, for all $v \in H^1(K)$, there holds*

$$\|v\|_{0,e}^2 \lesssim h^{-1}\|v\|_{0,K}^2 + h|v|_{1,K}^2.$$

Lemma 4 (A trace inequality on interface [71]) *On any interface element K, for all $v \in H^1(K)$, there holds*

$$\|v\|_{0,\Gamma_h^K} \lesssim h_K^{-1/2}\|v\|_{0,K} + h_K^{1/2}|v|_{1,K}. \tag{2.7}$$

Theorem 2.2 (Poincaré-Friedrichs' type inequalities [10, Lemma 6.8] and [8, (2.14)]) *Given a polygon K with Lipschitz boundary ∂K and the number of edges of K is uniformly bounded, for $v \in C^0(\partial K)$ and piecewise linear on ∂K, there holds, for each $e \subset \partial K$,*

$$\|v\|_{0,e} \lesssim h_K^{-1/2}\left|\int_{\partial K} v\,\mathrm{d}s\right| + h_K^{1/2}|v|_{1/2,\mathcal{E}_K}, \tag{2.8a}$$

where in the seminorm $|\cdot|_{1/2,\mathcal{E}_K}$ is defined in (5.3). Furthermore, if K is shape regular in the sense that it is star-shaped with respect to a disk with radius ρh_K, then for each $v \in H^1(K)$, there hold

$$\|v\|_{0,K} \lesssim \left|\int_{\partial K} v\,\mathrm{d}s\right| + h_K|v|_{1,K}. \tag{2.8b}$$

3 Immersed Virtual Element and Immersed Finite Element Spaces

In this section, we introduce the immersed virtual element (IVE) and the immersed finite element (IFE) spaces. Then we describe the associated projection and interpolation operators. We connect them by commuting diagrams.

3.1 Immersed Virtual Element Spaces

The proposed IVE space is a group of novel virtual element spaces with an interface immersed inside the element. As only the linear method is considered in this article, the interface is flattened inside each element, i.e., the whole interface is approximated by a polyline Γ_h. We let α_h and β_h be the piecewise constant coefficients with interface being Γ_h. As we only consider the lowest order methods, such a linear approximation to the geometry is sufficient.

3.1.1 H^1 Virtual Element Spaces

For each interface element K, we begin with an H^1 virtual element space that encodes the interface into its elements:

$$V_h^n(K) = \{v_h : \operatorname{div}(\beta_h \nabla v_h) = 0, \ \ v_h|_e \in \mathbb{P}_1(e), \ \forall e \in \mathcal{E}_K, \ \ v_h|_{\partial K} \in C^0(\partial K), \\ [v_h]_{\Gamma_h^K} = 0, \text{ and } [\beta_h \nabla v_h \cdot \bar{\mathbf{n}}]_{\Gamma_h^K} = 0\}. \tag{3.1}$$

Here we note that the jump conditions in (3.1) are imposed on the approximated interface Γ_h^K instead of on the exact interface Γ, the barred notation $\bar{\mathbf{n}}$ denotes the unit normal vector to Γ_h^K that points roughly in the same direction with $\mathbf{n}$. Similarly, $\bar{\mathbf{t}}$ is the unit tangential vector to Γ_h^K that is an approximation to $\mathbf{t}$. The motivation to impose the jump conditions on Γ_h^K is that the IFE space defined later becomes a subspace of $V_h^n(K)$, which facilitates a simpler analysis. There will be no essential difficulty if the jump conditions of the virtual element spaces are defined on Γ as the analysis follows the VEM meta-framework.

Clearly, $V_h^n(K)$ is not empty. The reason is that we can treat $V_h^n(K) \subseteq H^1(K)$ as the space of the weak solutions to a boundary value problem. Then, the dimension of $V_h^n(K)$ is that of the boundary conditions, i.e., the dimension of $\Pi_{e\in\mathcal{E}_K}\mathbb{P}_1(e) \cap C^0(\partial K)$, which further can be identified by the number of the vertices on ∂K. Consequently, $V_h^n(K)$ is unisolvent: if the DoFs $v_h(\mathbf{x}) = 0$ at each $\mathbf{x} \in \mathcal{N}_K$, which implies the boundary value $v_h = 0$ on ∂K, then $v_h \equiv 0$ in K by the uniqueness of the local problem. This space can be understood as a natural generalization of the classic linear virtual element space in [63, 65] to the case of discontinuous coefficients. Furthermore, referred to (1.6), we can see the space is also a generalization of 1D space by Babuška et al. in [5, 6].

Note that $V_h^n(K) \subset H^1(K) \cap \{\beta_h \nabla u \in \mathbf{H}(\operatorname{div}; K)\}$. Inside the interface element K, the piecewise constant function β_h serves as a Hodge star which maps the function $\nabla u \in \mathbf{H}(\operatorname{curl}; K)$ to a function $\beta_h \nabla u \in \mathbf{H}(\operatorname{div}; K)$.

The global space is then defined as

$$V_h^n = \{v_h \in H_0^1(\Omega) : v|_K \in V_h^n(K) \text{ if } K \in \mathcal{T}_h^i \text{ and } v|_K \in \mathbb{P}_1(K) \text{ if } K \in \mathcal{T}_h^n\} \tag{3.2}$$

which is an H^1-conforming space. Lastly, we can define the Lagrange type interpolation I_h^n using the nodal DoFs, for continuous u,

$$(I_h^n u)(\mathbf{x}) = u(\mathbf{x}), \qquad \forall \mathbf{x} \in \mathcal{N}_h. \tag{3.3}$$

3.1.2 H(curl) Virtual Element Spaces

Next, let us consider an $\mathbf{H}(\operatorname{curl})$ virtual element space involving discontinuous coefficients. Given an interface element K, we define

$$\mathbf{V}_h^e(K) = \{\mathbf{v}_h \in \mathbf{H}(\operatorname{curl}; K) : \ \beta_h \mathbf{v}_h \in \mathbf{H}(\operatorname{div}; K), \ \mathbf{v}_h \cdot \mathbf{t}_e|_e \in \mathbb{P}_0(e), \ \forall e \in \mathcal{E}_K, \\ \operatorname{div} \beta_h \mathbf{v}_h = 0, \ \alpha_h \operatorname{curl} \mathbf{v}_h \in \mathbb{P}_0(K)\}. \tag{3.4}$$

Again β_h is a Hodge star operator which maps $\mathbf{v}_h \in \mathbf{H}(\operatorname{curl}; K)$ to $\beta_h \mathbf{v}_h \in \mathbf{H}(\operatorname{div}; K)$ and α_h is another Hodge star which maps $\operatorname{curl} \mathbf{v}_h \in L^2(K)$ to $\alpha_h \operatorname{curl} \mathbf{v}_h \in H^1(K)$.

With this definition, it is easy to see

$$\operatorname{curl} \mathbf{V}_h^e(K) = \{c \text{ is a piecewise constant on } K_h^{\pm} : \ \alpha_h^+ c^+ = \alpha_h^- c^-\}. \tag{3.5}$$

In the rest of this section, we denote the weighted average of α on K by

$$\alpha_K = \left(|K_h^+|\alpha_h^- + |K_h^+|\alpha_h^+\right)/|K|. \tag{3.6}$$

If a piecewise constant vector $\mathbf{c} := \mathbf{c}^{\pm}$ on $K_h^{\pm}$ satisfies $\beta_h^+ \mathbf{c}^+ \cdot \bar{\mathbf{n}} = \beta_h^- \mathbf{c}^- \cdot \bar{\mathbf{n}}$ and $\mathbf{c}^+ \cdot \bar{\mathbf{t}} = \mathbf{c}^- \cdot \bar{\mathbf{t}}$, then $\mathbf{c} \in \mathbf{V}_h^e(K)$. Thus, $\mathbf{V}_h^e(K)$ is non-empty, and upon a closer inspection it is not hard to see that the aforementioned $\mathbf{c}^{\pm}$ form the gradient of the H^1 IFE space on K (see the definition of IFE spaces in Sect. 3.2.1). The dimension of $\mathbf{V}_h^e(K)$ is not immediately obvious. To characterize the functions in $\mathbf{V}_h^e(K)$, we consider the following local problem: given $f \in L^2(K)$ and $g \in L^2(\partial K)$, find $\mathbf{v}_h$ such that

$$\operatorname{curl} \mathbf{v}_h = f \quad \text{in } K, \tag{3.7a}$$

$$\operatorname{div}(\beta_h \mathbf{v}_h) = 0 \quad \text{in } K, \tag{3.7b}$$

$$\mathbf{v}_h \cdot \mathbf{t} = g \quad \text{on } \partial K. \tag{3.7c}$$

The following lemma establishes the well-posedness of this equation.

Lemma 5 *The equation in* (3.7) *is well-posed if the compatibility condition is met:*

$$\int_K f \, \mathrm{d}\mathbf{x} = \int_{\partial K} g \, \mathrm{d}s. \tag{3.8}$$

Proof By the constraint $\operatorname{div} \beta_h \mathbf{v}_h = 0$, the exact sequence property implies that there exists $\varphi \in H^1(K)$ such that $\mathbf{curl}\, \varphi = \beta_h \mathbf{v}_h$. Then the argument basically mimics the one in the proof of Lemma 1 locally on an element. In particular, the problem (3.7) then becomes a pure Neumann problem:

$$\operatorname{curl}(\beta_h^{-1} \mathbf{curl}\, \varphi) = -\operatorname{div}(\beta_h^{-1} \nabla \varphi) = f \quad \text{in } K, \tag{3.9a}$$

$$\beta_h^{-1} \nabla \varphi \cdot \mathbf{n} = -g \quad \text{on } \partial K. \tag{3.9b}$$

Clearly, for any boundary condition g and source term f satisfying the compatibility condition (3.8), (3.9) has a unique solution $\varphi \in H^1(K)/\mathbb{R}$, and thus a unique $\mathbf{v}_h = \beta_h^{-1} \mathbf{curl}\, \varphi$. □

We then follow [17] to introduce the so-called data space

$$\mathcal{D}(K) = \{(f_0, g_0) : \alpha_h f_0 \in \mathbb{P}_0(K),\, g_0|_e \in \mathbb{P}_0(e),\, e \in \mathcal{E}_K,\ \text{and} \int_K f_0 \, \mathrm{d}\mathbf{x} = \int_{\partial K} g_0 \, \mathrm{d}s.\}$$

Despite the fact f_0 gives an extra 1 dimension, the compatible condition reduces this extra dimension, and thus $\dim \mathcal{D}(K) = |\mathcal{E}_K|$. Given a function $\mathbf{u} \in \mathbf{V}_h^e(K)$, $(\operatorname{curl} \mathbf{v}_h, \mathbf{v}_h \cdot \mathbf{t}_{\partial K})$ defines a mapping $\mathcal{L} : \mathbf{V}_h^e(K) \to \mathcal{D}(K)$. On the other hand, given $(f_0, g_0) \in \mathcal{D}(K)$, the solution $\mathbf{v}_h$ to the local problem (3.7) is a function in $\mathbf{V}_h^e(K)$. The uniqueness of the local problem implies $\mathcal{L}^{-1}$ is well-defined. Therefore, $\mathcal{L}$ is one-to-one, and $\dim \mathbf{V}_h^e(K) = \dim \mathcal{D}(K) = |\mathcal{E}_K|$. Next we show the DoFs on the edges in $\mathcal{E}_K$ suffice to uniquely determine a function in $\mathbf{V}_h^e(K)$ as follows.

Lemma 6 *The DoFs* $\{\mathbf{v}_h \cdot \mathbf{t}_e, e \in \mathcal{E}_K\}$ *are unisolvent on the space* $\mathbf{V}_h^e(K)$ *for any* $K \in \mathcal{T}_h$.

Proof First of all, the number of DoFs $\{\mathbf{v}_h \cdot \mathbf{t}_e, e \in \mathcal{E}_K\}$ is $|\mathcal{E}_K|$ which is equal to the dimension of the space $\mathbf{V}_h^e(K)$. Then, a mapping can be defined from DoFs to the data space $\mathcal{D}(K)$. An obvious choice is $g_0|_e = \mathbf{v}_h \cdot \mathbf{t}_e \in \mathbb{P}_0(e)$. From the compatibility condition

$$\sum_{e \in \mathcal{E}_K} |e| \mathbf{v}_h \cdot \mathbf{t}_e = \int_{\partial K} \mathbf{v}_h \cdot \mathbf{t} \, \mathrm{d}s = \int_K \operatorname{curl}\, \mathbf{v}_h \, \mathrm{d}\mathbf{x} = |K_h^+| (\operatorname{curl} \mathbf{v}_h)^+ + |K_h^-| (\operatorname{curl} \mathbf{v}_h)^-, \tag{3.10}$$

where $(\operatorname{curl} \mathbf{v}_h)^{\pm}$ are constant restricted to $K_h^{\pm}$, respectively. On the other hand, by definition of the space, we have equation

$$\alpha_h^+ (\operatorname{curl} \mathbf{v}_h)^+ = \alpha_h^- (\operatorname{curl} \mathbf{v}_h)^-. \tag{3.11}$$

Then solve (3.10)-(3.11) for $(\operatorname{curl} \mathbf{v}_h)^{\pm}$, which are two constant scalars, we get

$$(\operatorname{curl} \mathbf{v}_h)^+ = \frac{1}{|K|} \frac{\alpha_h^-}{\alpha_K} \int_{\partial K} \mathbf{v}_h \cdot \mathbf{t} \, \mathrm{d}s, \quad (\operatorname{curl} \mathbf{v}_h)^- = \frac{1}{|K|} \frac{\alpha_h^+}{\alpha_K} \int_{\partial K} \mathbf{v}_h \cdot \mathbf{t} \, \mathrm{d}s, \tag{3.12}$$

where the weighted average α_K is given in (3.6). That is to say, the second output of this map in $\mathcal{D}(K)$, $f_0 = \operatorname{curl} \mathbf{v}_h$ can be expressed by a linear combination of DoFs. Therefore, the unisolvence follows from the uniqueness of the local problem (3.7). More precisely, if $\mathbf{v}_h \cdot \mathbf{t}_e$ vanishes for every $e \in \mathcal{E}_K$, then both f_0 and g_0 are zero and consequently the solution $\mathbf{v}_h$ to (3.7) is zero. □

The importance of this lemma is that we have established the one-to-one correspondance between the local virtual element space, the DoFs, and the data space. Moreover, from the proof, curl $\mathbf{v}_h$ is readily computable for any $\mathbf{v}_h \in \mathbf{V}_h^e(K)$ through the DoFs using (3.12), which is vital for the implementation.

Thanks to the edge DoFs, we can also construct a globally $\mathbf{H}(\operatorname{curl})$-conforming space

$$\mathbf{V}_h^e = \{\mathbf{v}_h \in \mathbf{H}(\operatorname{curl}; \Omega) : \mathbf{v}_h|_K \in \mathbf{V}_h^e(K) \text{ if } K \in \mathcal{T}_h^i \text{ and } \mathbf{v}_h|_K \in \mathcal{ND}_0(K) \text{ if } K \in \mathcal{T}_h^n\}. \tag{3.13}$$

We can define the edge interpolation $I_h^e \mathbf{u}$ as, provided that $\mathbf{u}$ is smooth enough,

$$\int_e I_h^e \mathbf{u} \cdot \mathbf{t} \, \mathrm{d}s = \int_e \mathbf{u} \cdot \mathbf{t} \, \mathrm{d}s, \qquad \forall e \in \mathcal{E}_h. \tag{3.14}$$

3.1.3 H(div) Virtual Element Spaces

Similarly, given an interface element K, the $\mathbf{H}(\operatorname{div})$ virtual element space involving discontinuous coefficients is defined as

$$\begin{aligned} \mathbf{V}_h^f(K) = \{\mathbf{v}_h \in \mathbf{H}(\operatorname{div}; K) : \beta_h^{-1} \mathbf{v}_h \in \mathbf{H}(\operatorname{curl}; K), \ \mathbf{v}_h \cdot \mathbf{n}_e \in \mathbb{P}_0(e), \ \forall e \in \mathcal{E}_K, \\ \operatorname{div} \mathbf{v}_h \in \mathbb{P}_0(K), \ \operatorname{curl} \beta_h^{-1} \mathbf{v}_h = 0\}. \end{aligned} \tag{3.15}$$

Different from the standard virtual element spaces, $\mathbf{V}_h^f(K)$ is not exactly the rotation of $\mathbf{V}_h^e(K)$. Indeed, the Hodge star is defined by β_h^{-1} which maps a function $\mathbf{v}_h \in \mathbf{H}(\operatorname{div}; K)$ to $\beta_h^{-1} \mathbf{v}_h \in \mathbf{H}(\operatorname{curl}; K)$.

By a similar argument to Sect. 3.1.2 that leads to Lemma 6, we can show that the definition (3.15) yields a well-defined local space with DoFs being $\mathbf{v}_h \cdot \mathbf{n}_e$, $\forall e \in \mathcal{E}_K$, and thus has the dimension $|\mathcal{E}_K|$. Similarly, $\operatorname{div} \mathbf{v}_h$, $\mathbf{v}_h \in \mathbf{V}_h^f(K)$ is computable using these DoFs through the integration by parts:

$$|K| \operatorname{div} \mathbf{v}_h = \int_K \operatorname{div} \mathbf{v}_h \, \mathrm{d}\mathbf{x} = \int_{\partial K} \mathbf{v}_h \cdot \mathbf{n} \, \mathrm{d}s. \tag{3.16}$$

Then, the global $\mathbf{H}(\operatorname{div})$ virtual element space is

$$\mathbf{V}_h^f = \{\mathbf{v}_h \in \mathbf{H}(\operatorname{div}; \Omega) : \mathbf{v}_h|_K \in \mathbf{V}_h^f(K) \text{ if } K \in \mathcal{T}_h^i \text{ and } \mathbf{v}_h|_K \in \mathcal{RT}_0(K) \text{ if } K \in \mathcal{T}_h^n\}. \tag{3.17}$$

We can also define the edge interpolation $I_h^f \mathbf{u}$ as, provided $\mathbf{u}$ is smooth enough,

$$\int_e I_h^f \mathbf{u} \cdot \mathbf{n} \, \mathrm{d}s = \int_e \mathbf{u} \cdot \mathbf{n} \, \mathrm{d}s, \qquad \forall e \in \mathcal{E}_h. \tag{3.18}$$

We note that both I_h^e and I_h^f are just standard edge interpolation on non-interface elements.

3.1.4 A discrete de Rham Complex

The commuting diagram and a discrete de Rham complex also hold for the newly constructed virtual element spaces. Given each element K and a weight function $w \in L^2(K)$ that is piecewise constant $w^{\pm}$ on $K_h^{\pm}$, let π_K^w be the projection, defined with the inner product $(w\cdot, \cdot)_K$, onto

$$Q_h^w(K) = \{c \text{ is a piecewise constant on } K_h^{\pm} : \ w^+ c^+ = w^- c^-\}. \tag{3.19}$$

Namely, for $z \in L^2(K)$ there holds

$$(w \, \pi_K^w z, v)_K = (w \, z, v)_K, \quad \forall v \in Q_h^w(K). \tag{3.20}$$

In particular, if K is simply a non-interface element or $w = 1$, π_K^w reduces to the standard L^2 projection onto $Q_h^1(K) = \mathbb{P}_0(K)$. If K is an interface element and $w = \alpha_h$, from (3.5) we have $Q_h^{\alpha_h}(K) = \operatorname{curl} \mathbf{V}_h^e(K)$.

We first summarize the aforementioned Hodge star operators associated with $V_h^n(K)$ and $\mathbf{V}_h^e(K)$ through the following diagram

$$\begin{array}{ccccccccc} \mathbb{R} & \longrightarrow & V_h^n(K) & \xrightarrow{\nabla} & \mathbf{V}_h^e(K) & \xrightarrow{\operatorname{curl}} & Q_h^{\alpha_h}(K) & \longrightarrow & 0 \\ & & \downarrow I & & \downarrow \beta_h & & \downarrow \alpha_h & & \\ 0 & \longleftarrow & L^2(K) & \xleftarrow{\operatorname{div}} & \mathbf{H}(\operatorname{div}; K) & \xleftarrow{\operatorname{curl}} & H^1(K) & \longleftarrow & \mathbb{R}. \end{array} \tag{3.21}$$

We note that this diagram exactly mimics the one in (2.2) which shows the proposed spaces nicely inherit this feature locally on interface elements.

Furthermore, given $w \in L^2(\Omega)$ that is piecewise constant weight function on each element and subelement of interface elements, we let Q_h^w be a piecewise constant space satisfying $Q_h^w|_K = Q_h^w(K)$. Let the global projection be $\pi_h^w|_K = \pi_K^w$. Then, we have our diagram in (1.5). Let us proceed to show its exactness and commutative property.

Lemma 7 *There holds*

$$\nabla V_h^n \subset \mathbf{V}_h^e \cap \operatorname{Ker}(\operatorname{curl}).$$

Consequently, together with $\operatorname{curl} \mathbf{V}_h^e = Q_h^{\alpha_h}$*, the discrete sequence on the bottom of (1.5) is a complex.*

Proof We first show the local subset result and focus on interface elements K, since the argument for non-interface elements is standard. Given $v_h \in V_h^n(K)$, $[v_h]_{\Gamma_h^K} = 0$ and $[\beta_h \nabla v_h \cdot \tilde{\mathbf{n}}]_{\Gamma_h^K} = 0$ imply $\nabla v_h \in \mathbf{H}(\operatorname{curl}; K)$ and $\beta_h \nabla v_h \in \mathbf{H}(\operatorname{div}; K)$, respectively. In addition, we also have $\operatorname{div}(\beta_h \nabla v_h) = 0$ by the local problem (3.7). Besides, $v_h|_e \in \mathbb{P}_1(e)$ implies $\nabla v_h|_e \cdot \mathbf{t} \in \mathbb{P}_0(e)$. Moreover, it is trivial that $\operatorname{curl}(\nabla v_h) = 0$ which gives the desired local subset result. It leads to the global one by their DoFs. □

Lemma 8 *The discrete sequence on the bottom of* (1.5)*, is exact.*

Proof Given $\mathbf{v}_h \in \mathbf{V}_h^e \cap \mathrm{Ker}(\mathrm{curl})$, there exists a $\varphi_h \in H^1(\Omega)$ such that $\nabla\varphi_h = \mathbf{v}_h$ by the continuous exact sequence. We need to show $\varphi_h \in V_h^n$. On non-interface elements K, as $\mathbf{v}_h$ is a constant vector, there simply holds $\varphi_h \in \mathbb{P}_1(K)$. On any $K \in \mathcal{T}_h^i$, as $\mathrm{div}(\beta_h\mathbf{v}_h) = 0$, we also have $-\nabla\cdot(\beta_h\nabla\varphi_h) = 0$. The jump conditions for φ_h are thus satisfied due to those of $\mathbf{v}_h$. It follows from the DoFs $\mathbf{v}_h\cdot\mathbf{t} = \nabla\varphi_h\cdot\mathbf{t} \in \mathbb{P}_0(e)$ that $\varphi_h \in \mathbb{P}_1(e)$, $\forall e \in \mathcal{E}_K$. These results lead to $\varphi_h \in V_h^n(K)$. Thus, we have $\varphi_h \in V_h^n$ through their DoFs.

To show curl is surjective, we construct an auxiliary mesh $\mathcal{T}_h^A$ by simply refining interface elements into several triangles. Given $q_h \in Q_h^{\alpha_h} \subset H^1(\alpha_h;\mathcal{T}_h)$, it is trivial that q_h can be considered as a piecewise constant function on $\mathcal{T}_h^A$. Then, the classic exact sequence yields a curl-conforming Nédélec element $\tilde{\mathbf{w}}_h \in \mathbf{H}(\mathrm{curl};\Omega)$ with $\tilde{\mathbf{w}}_h|_K \in \mathcal{ND}_0(K)$, $\forall K \in \mathcal{T}_h^A$ such that curl $\tilde{\mathbf{w}}_h = q_h$. We set $\mathbf{w}_h = I_h^e\tilde{\mathbf{w}}_h \in \mathbf{V}_h^e$, that is, their edge moments only have to agree on the edges in $\mathcal{E}_h$, not on the extra interior edges to form $\mathcal{T}_h^A$. It is trivial that curl $\mathbf{w}_h =$ curl $\tilde{\mathbf{w}}_h = q_h$ on $K \in \mathcal{T}_h^n$. We only need to verify it on interface elements. Given $K \in \mathcal{T}_h^i$, we let $q_h^{\pm} = q_h|_{K^{\pm}}$. With integration by parts, there holds $\int_K$ curl $\tilde{\mathbf{w}}_h\,\mathrm{d}\mathbf{x} = \int_{\partial K}\tilde{\mathbf{w}}_h\cdot\mathbf{t}\,\mathrm{d}s$. Then, by $\alpha^+q_h^+ = \alpha^-q_h^-$ we have

$$q_h^{\pm} = \frac{1}{|K|}\frac{\alpha_h^{\mp}}{\alpha_K}\int_{\partial K}\tilde{\mathbf{w}}_h\cdot\mathbf{t}\,\mathrm{d}s = \frac{1}{|K|}\frac{\alpha_h^{\mp}}{\alpha_K}\int_{\partial K}\mathbf{w}_h\cdot\mathbf{t}\,\mathrm{d}s$$

with α_K defined in (3.6). Using (3.12), we have concluded curl $\mathbf{w}_h = q_h$. □

Remark 2 The global Nédélec edge element constructed in the proof above can be understood as a function in the virtual element space developed in [12] with discontinuous coefficients, in which the DoFs associated with the interior edges of an interface element are eliminated by imposing a single constant curl value.

Note that for standard FEM on non-interface elements, curl $I_h^e\mathbf{u}$ is the projection of curl $\mathbf{u}$ onto the constant space, which is the well-known commuting property for the de Rham complex. For the new virtual element spaces, the commuting property also holds.

Lemma 9 *The diagram in* (1.5) *is commutative.*

Proof It suffices to establish the result on interface elements. To this end, given one interface element K, we shall first show for any $u \in H^2(\beta;\mathcal{T}_h)$, there holds

$$I_h^e\nabla u = \nabla I_h^n u. \tag{3.22}$$

As shown in Lemma 7, we have $\nabla I_h^n u \in \mathbf{V}_h^e(K)$; so by the unisolvence in Lemma 6, to prove (3.22), it remains to check their DoFs coincide. Indeed, given each $e \in \mathcal{E}_K$ with the ending points $\mathbf{a}_e$ and $\mathbf{b}_e$, we have

$$\int_e \nabla I_h^n u\cdot\mathbf{t}\,\mathrm{d}s = I_h^n u(\mathbf{a}_e) - I_h^n u(\mathbf{b}_e) = u(\mathbf{a}_e) - u(\mathbf{b}_e) = \int_e \nabla u\cdot\mathbf{t}\,\mathrm{d}s = \int_e I_h^e\nabla u\cdot\mathbf{t}\,\mathrm{d}s.$$

Furthermore, we need to show for any $\mathbf{u} \in \mathbf{H}^1(\mathrm{curl},\alpha,\beta;\mathcal{T}_h)$, there holds

$$\mathrm{curl}\ I_h^e\mathbf{u} = \pi_K^{\alpha_h}\,\mathrm{curl}\ \mathbf{u}. \tag{3.23}$$

Note that functions in $Q_h^{\alpha_h}(K)$ are simply $\alpha_h^{-1}c$ with any constant c. Then, Green's theorem gives

$$\begin{aligned}\int_K \alpha_h\,\mathrm{curl}\,I_h^e\mathbf{u}\,\alpha_h^{-1}c\,\mathrm{d}\mathbf{x} &= \int_K \mathrm{curl}\,I_h^e\mathbf{u}\,c\,\mathrm{d}\mathbf{x} = c\int_{\partial K} I_h^e\mathbf{u}\cdot\mathbf{t}\,\mathrm{d}s\\ = c\int_{\partial K}\mathbf{u}\cdot\mathbf{t}\,\mathrm{d}s &= \int_K \mathrm{curl}\,\mathbf{u}\,c\,\mathrm{d}\mathbf{x} = \int_K \alpha_h\,\mathrm{curl}\,\mathbf{u}\,\alpha_h^{-1}c\,\mathrm{d}\mathbf{x},\end{aligned} \tag{3.24}$$

which yields the desired result. □

Remark 3 It is highlighted that the commutative property essentially only depends on the DoFs of the IVE spaces. It makes the definition of IVE spaces quite flexible. For example, the property still holds if the IVE spaces are defined with the original interface Γ instead of the approximate interface Γ_h, if appropriate jump conditions are imposed on Γ.

Here we assume higher regularity for the spaces in the continuous level so that the canonical interpolation operator I_h^n and I_h^e are well-defined. In the rest of this article, we simply denote these interpolations by

$$u_I := I_h^n u \quad \text{and} \quad \mathbf{u}_I := I_h^e \mathbf{u}, \tag{3.25}$$

if there is no confusion. It is possible to follow the approach in [27, 62] to construct quasi-interpolation operators without extra smoothness requirement and establish the commutative property.

3.2 Immersed Finite Element Spaces

Similar to the standard VEM [63, 65], the basis functions themselves in the virtual element space do not have explicit pointwise values for computation, and this demands projections. Due to jump conditions, the standard polynomial spaces are not appropriate choices onto which the virtual element spaces are projected. As the IFE space consists of piecewise polynomials satisfying the jump conditions on Γ_h^K, naturally it can be used as a computable space for projecting. To simplify the discussion, starting from this section, we only consider the interface element in Fig. 2a; namely, we make the following assumption:

Assumption 3.1 (The background mesh being fine enough) For each interface triangle K in the background mesh, Γ intersects with K at most two distinct points on two different edges.

We note that this assumption can be satisfied if $\mathcal{T}_h$ is sufficiently fine [23, 28] provided that $\Gamma \in C^{1,1}$, i.e., the interface is locally flat enough. Even if the interface intersects an element multiple times, such as Fig. 2b and c, the proposed method is still applicable, since the immersed virtual functions always exist from solving local problems, which is one of the major difference from the conventional IFEM. So, this assumption is merely to simplify the analysis. Now, let us review three types of IFE spaces including the H^1, $\mathbf{H}(\text{curl})$, and $\mathbf{H}(\text{div})$ spaces.

3.2.1 H^1 IFE Spaces

First, we consider the H^1 case, see e.g., [30]. Given an interface element K, we consider the approximate jump conditions to (1.2) defined on the segment Γ_h^K:

$$v_h^+ = v_h^- \qquad \text{at } \Gamma_h^K, \tag{3.26a}$$

$$\beta_h^+ \nabla v_h^+ \cdot \bar{\mathbf{n}} = \beta_h^- \nabla v_h^- \cdot \bar{\mathbf{n}} \qquad \text{at } \Gamma_h^K. \tag{3.26b}$$

Note that (3.26a) leads to $\nabla v_h^+ \cdot \bar{\mathbf{t}} = \nabla v_h^- \cdot \bar{\mathbf{t}}$, which together with (3.26b) leads to the relation

$$\nabla v_h^+ = M \nabla v_h^- \quad , \tag{3.27}$$

where M is an invertible matrix encoded with the jump information

$$M = \begin{bmatrix} n_2^2 + \rho n_1^2 & (\rho - 1)n_1 n_2 \\ (\rho - 1)n_1 n_2 & n_1^2 + \rho n_2^2 \end{bmatrix} \tag{3.28}$$

with $\bar{\mathbf{n}} = (n_1, n_2)$, $\bar{\mathbf{t}} = (t_1, t_2) = (n_2, -n_1)$, and $\rho = \beta^-/\beta^+$. Accordingly, we can express the H^1 IFE functions explicitly as follows:

$$v_h(\mathbf{x}) = \begin{cases} M\mathbf{c} \cdot (\mathbf{x} - \mathbf{x}^m) + c_0 & \text{if } \mathbf{x} \in K_h^+, \\ \mathbf{c} \cdot (\mathbf{x} - \mathbf{x}^m) + c_0 & \text{if } \mathbf{x} \in K_h^-, \end{cases} \tag{3.29}$$

where $\mathbf{x}^m = (x_1^m, x_2^m)^\intercal$ is the mid-point of Γ_h^K, and c_0 and $\mathbf{c}$ are scalar- and vector-valued constants that can be viewed as the DoFs for the polynomial space. Now, the H^1 local IFE space on K is then defined as

$$S_h^n(K) := \{v_h|_{K_h^\pm} \in \mathbb{P}_1(K_h^\pm) : \ v_h \text{ satisfies (3.26)}\}. \tag{3.30}$$

By counting the number of constraints, $\dim S_h^n(K) = 3$. Comparing it with the virtual element space (3.1), it is straightforward to conclude that $S_h^n(K) \subset V_h^n(K)$. In the classical definition of IFE, e.g. [28], the IFE space admits the DoFs as the values at the vertices of a triangular element K. In contrast, this nodal basis–DoF pair is now different, as the DoFs are imposed through the virtual element space. Note that the IFE basis in (3.29) is not the conventional nodal IFE basis, and the formula in (3.29) is easier to be derived and only used for computing projections.

3.2.2 H(curl) IFE Spaces

The $\mathbf{H}(\text{curl})$ IFE space is developed in [31] which employs the approximate jump conditions for piecewise polynomials $\mathbf{v}_h^\pm \in \mathcal{ND}_0(K_h^\pm)$

$$\mathbf{v}_h^+ \cdot \bar{\mathbf{t}} = \mathbf{v}_h^- \cdot \bar{\mathbf{t}} \qquad \text{at } \Gamma_h^K, \tag{3.31a}$$

$$\alpha_h^+ \operatorname{curl} \mathbf{v}_h^+ = \alpha_h^- \operatorname{curl} \mathbf{v}_h^- \qquad \text{at } \Gamma_h^K, \tag{3.31b}$$

$$\beta_h^+ \mathbf{v}_h^+ \cdot \bar{\mathbf{n}} = \beta_h^- \mathbf{v}_h^- \cdot \bar{\mathbf{n}} \qquad \text{at } \mathbf{x}^m. \tag{3.31c}$$

Then, the $\mathbf{H}(\text{curl})$ IFE space is defined as

$$\mathbf{S}_h^e(K) = \{\mathbf{v}_h|_{K_h^\pm} \in \mathcal{ND}_0(K_h^\pm) \ : \ \mathbf{v}_h \text{ satisfies (3.31)}\}. \tag{3.32}$$

The functions in $\mathbf{S}_h^e(K)$ admit the following explicit representation:

$$\mathbf{v}_h = \begin{cases} M\mathbf{c} + \frac{c_0}{\alpha^+}(-(x_2 - x_2^m), x_1 - x_1^m)^\intercal & \text{in } K_h^+, \\ \mathbf{c} + \frac{c_0}{\alpha^-}(-(x_2 - x_2^m), x_1 - x_1^m)^\intercal & \text{in } K_h^-, \end{cases} \tag{3.33}$$

where M is given by (3.28), and c_0 and $\mathbf{c}$ are arbitrary scalar- and vector-valued constants.

3.2.3 H(div) IFE Spaces

To derive a systematic framework, we also recall the $\mathbf{H}(\text{div})$ IFE space [42] which is used to approximate $\beta\nabla u \in \mathbf{H}(\text{div}; K)$. The related approximate jump conditions are defined as

$$\mathbf{v}_h^+ \cdot \bar{\mathbf{n}} = \mathbf{v}_h^- \cdot \bar{\mathbf{n}} \qquad \text{on } \Gamma_h^K, \tag{3.34a}$$

$$(\beta_h^+)^{-1}\mathbf{v}_h^+ \cdot \bar{\mathbf{t}} = (\beta_h^-)^{-1}\mathbf{v}_h^- \cdot \bar{\mathbf{t}}, \qquad \text{at } \mathbf{x}^m. \tag{3.34b}$$

together with the condition

$$\operatorname{div} \mathbf{v}_h^+ = \operatorname{div} \mathbf{v}_h^-. \tag{3.34c}$$

We note that (3.34c) is proposed in [42] for guaranteeing unisolvence, but it is interesting to note that it also mimics the condition of the face IVE space in (3.15), i.e. div v_h is a single constant in K. We emphasize again that the jump condition is from the discrete Hodge star β_h^{-1} which maps $\mathbf{v}_h \in \mathbf{H}(\text{div}; K)$ to $\beta_h^{-1}\mathbf{v}_h \in \mathbf{H}(\text{curl}; K)$.

Then, the $\mathbf{H}(\text{div})$ IFE space is defined as

$$\mathbf{S}_h^f(K) = \{\mathbf{v}_h|_{K_h^\pm} \in \mathcal{RT}_0(K_h^\pm) \ : \ \mathbf{v}_h \text{ satisfies (3.34)}\}. \tag{3.35}$$

Again, we can derive the explicit formulas for functions in $\mathbf{S}_h^f(K)$:

$$\mathbf{v}_h = \begin{cases} M'\mathbf{c} + c_0(\mathbf{x} - \mathbf{x}^m) & \text{in } K_h^+, \\ \mathbf{c} + c_0(\mathbf{x} - \mathbf{x}^m) & \text{in } K_h^-, \end{cases} \tag{3.36}$$

where c_0 and $\mathbf{c}$ are arbitrary scalar- and vector-valued constants, and $M' = \rho^{-1}M$.

Remark 4 Comparing the virtual element space (3.4) and the IFE space (3.32), we find that the only difference is that $\beta_h\mathbf{v}_h \notin \mathbf{H}(\text{div}; K)$ for $\mathbf{v}_h \in \mathbf{S}_h^e(K)$, since the normal continuity only holds at one point $\mathbf{x}^m$ as shown in (3.31c). Thus, $\mathbf{S}_h^e(K) \not\subset \mathbf{V}_h^e(K)$ which is different from the H^1 case. Similarly, for the $\mathbf{H}(\text{div})$ case, we still do not have $\mathbf{S}_h^f(K) \not\subset \mathbf{V}_h^f(K)$ since the tangential continuity only holds at $\mathbf{x}^m$. Note that the similar practices occur in the VEM literature. For example, the serendipity VEM spaces often use DoFs/projections as constraints in the definition of the virtual element spaces to eliminate interior DoFs, e.g., [64, 70]. However, due to the presence geometry-tied constraints such as the barycenter in the space definition, some common constructions for the vector polynomial space may not directly yield a subspace of this serendipity-type space anymore. Nevertheless, the flexibility of the VEM framework still guarantees convergence for a class of admissible geometry-tied constraints if the polynomial space offers approximation, e.g., see the discussion in [13, Appendix]. Another example is VEM on curved edges or faces, e.g., [69], the exact geometry is captured by the virtual element spaces that does not contain the standard polynomial spaces, and the projection is done in an isogeometric fashion to guarantee the approximation to geometry. As for the present case, the IVE spaces contain a piecewise constant vector proper subspace of the IFE spaces, onto which the IVE functions are then projected. This is sufficient for an optimal first order accuracy.

3.2.4 The Exact Sequence for IFE Spaces

First of all, it is not hard to see

$$\operatorname{curl} \mathbf{V}_h^e = \operatorname{curl} \mathbf{S}_h^e(K) = Q_h^{\alpha_h}(K) \quad \text{and} \quad \operatorname{div} \mathbf{V}_h^f = \operatorname{div} \mathbf{S}_h^e(K) = Q_h^1(K). \tag{3.37}$$

Let us recall the discrete de Rham complex and exact sequence for IFE spaces which will be useful in the later discussion. Here, we only need the local ones: [31, Theorem 3.5] shows

$$\mathbb{R} \xrightarrow{\hookrightarrow} S_h^n(K) \xrightarrow{\nabla} \mathbf{S}_h^e(K) \xrightarrow{\text{curl}} Q_h^{\alpha_h}(K) \to 0. \tag{3.38}$$

A similar exact sequence is

$$\mathbb{R} \xrightarrow{\hookrightarrow} \widetilde{S}_h^n(K) \xrightarrow{\mathbf{curl}} \mathbf{S}_h^f(K) \xrightarrow{\text{div}} Q_h^1(K) \to 0. \tag{3.39}$$

Here, $\widetilde{S}_h^n(K)$ is an H^1 IFE spaces but with the parameter β_h^{-1} and a rotated gradient, i.e., (3.26) is replaced by

$$(\beta_h^+)^{-1}\mathbf{curl} v_h^+ \cdot \bar{\mathbf{t}} = (\beta_h^-)^{-1}\mathbf{curl} v_h^- \cdot \bar{\mathbf{t}} \quad \text{on } \Gamma_h^K. \tag{3.40}$$

We mention that $\mathbf{S}_h^f(K)$ is the space used in [42] for mixed IFE methods. Then, we have the following result.

Lemma 10 *The Hodge star operator $\beta_h \cdot$ induces a one-to-one mapping from $\nabla S_h^n(K)$ to* $\mathbf{curl}\, \widetilde{S}_h^n(K)$*:*

$$\beta_h \nabla S_h^n(K) = \mathbf{curl}\, \widetilde{S}_h^n(K). \tag{3.41}$$

Proof For a function $v_h \in S_h^n(K)$, ∇v_h is a piecewise constant vector in $\mathbf{H}(\text{curl}; K)$, i.e., with tangential continuity. By construction $\beta_h \nabla v_h \in \mathbf{S}_h^f(K)$ is a piecewise constant vector but now continuous at normal direction. Therefore, $\text{div}\, \beta_h \nabla v = 0$. So we have proved $\beta_h \nabla S_h^n(K) \subseteq \text{Ker}(\text{div}) \cap \mathbf{S}_h^f(K) = \mathbf{curl}\, \widetilde{S}_h^n(K)$. By the same argument but switching $S_h^n(K)$ and $\widetilde{S}_h^n(K)$, we have $\beta_h^{-1}\mathbf{curl}\, \widetilde{S}_h^n(K) \subseteq \text{Ker}(\text{curl}) \cap \mathbf{S}_h^e(K) = \nabla S_h^n(K)$. This finishes the proof. □

Remark 5 Lemma 5 shows for each $\mathbf{v}_h \in \mathbf{V}_h^e$, there uniquely exists $\varphi_h \in H^1(K)$ such that $\beta_h^{-1}\mathbf{curl}\, \varphi_h = \mathbf{v}_h$ and $\int_{\partial K} \varphi_h \, \mathrm{d}s = 0$. If $\mathbf{v}_h$ is assumed to be a constant vector whose divergence vanishes, then by sequence (3.39) $\varphi_h \in \widetilde{S}_h^n(K)$. Moreover, with the Poincaré-Friedrichs' inequality (2.8b) and the trace inequality in Lemma 3, we can show the stability:

$$h_K^{1/2}\|\varphi_h\|_{0,\partial K} + \|\varphi_h\|_{0,K} \lesssim h_K \|\mathbf{v}_h\|_{0,K}. \tag{3.42}$$

3.3 Projections

It can be shown that the IFE spaces $S_h^n(K)$, $\mathbf{S}_h^e(K)$ and $\mathbf{S}_h^f(K)$ are unisolvent by the nodal DoFs [28], edge DoFs $\int_e \mathbf{v}_h \cdot \mathbf{t}\, \mathrm{d}s$ [31] and $\int_e \mathbf{v}_h \cdot \mathbf{n}\, \mathrm{d}s$ [42], respectively. These DoFs are critical for the conventional IFE methods in both analysis and computation. Proofs of the unisolvence with respect to the DoFs are generally very technical and rely on mesh assumption, for example the "no-obtuse-angle" condition introduced in [31, 42]. For some other problems, the unisolvence may not even hold, such as the elasticity problem [29], or the case that the interface intersects an element multiple times. It is highlighted that both the analysis and implementation of the proposed method do not rely on the unisolvence of the DoFs for the IFE spaces themselves, as they only serve as a computable projection space of the underlying virtual element spaces that offers a sufficient approximation power. IFE is used locally and thus no inter-element continuity is needed. Roughly speaking, the usual IFE shape functions will be replaced by a certain projection of ϕ_h to IFE spaces, where ϕ_h's are the shape functions of the virtual element spaces. This is one of the major difference of the proposed method from those classical IFE works. With this property, the IVEM is more flexible and generalizable.

Let us describe how to compute the projection from the IVE spaces to the IFE spaces. For the H^1 case, we introduce a projection $\Pi_K^{\beta_h} : H^1(K) \to S_h^n(K)$:

$$(\beta_h \nabla \Pi_K^{\beta_h} u, \nabla v_h)_K = (\beta_h \nabla u, \nabla v_h)_K, \quad \forall v_h \in S_h^n(K), \quad \text{and} \int_{\partial K} \left(u - \Pi_K^{\beta_h} u_h\right) \mathrm{d}s = 0.$$

(3.43)

By the continuity of $u_h \in V_h^n(K)$ and flux jump condition of $v_h \in S_h^n(K)$, applying integration by parts, we have

$$\int_K \beta_h \nabla u_h \cdot \nabla v_h \, \mathrm{d}\mathbf{x} = \int_{\partial K} \beta_h u_h \nabla v_h \cdot \mathbf{n} \, \mathrm{d}s, \tag{3.44}$$

which is computable, since $u_h|_{\partial K}$ is explicitly known, and $v_h \in S_h^n(K)$ can have its gradient evaluated explicitly. Therefore $\Pi_K^{\beta_h} u_h$ for a VEM function $u_h \in V_h^n(K)$ is computable. This projection exactly mimics the usual one used in the VEM literature.

For the $\mathbf{H}(\mathrm{curl})$ interface problem, as curl $\mathbf{v}_h$ is explicitly computable through the DoFs, cf. (3.12), but not $\mathbf{v}_h$. As a result, we only need to approximate the L^2 term. To this end, a weighted L^2 projection is introduced $\mathbf{\Pi}_K^{\beta_h} : L^2(K) \to \nabla S_h^n(K)$. For $\mathbf{u} \in L^2(K)$, $\beta_h \mathbf{\Pi}_K^{\beta_h} \mathbf{u} \in \nabla S_h^n(K)$ such that

$$(\beta_h \mathbf{\Pi}_K^{\beta_h} \mathbf{u}, \mathbf{v}_h)_K = (\beta_h \mathbf{u}, \mathbf{v}_h)_K, \quad \forall \mathbf{v}_h \in \nabla S_h^n(K). \tag{3.45}$$

Since $\mathbf{v}_h \in \nabla S_h^n(K)$, by (3.41) we have $\beta_h \mathbf{v}_h \in \beta_h \nabla S_h^n(K) = \mathbf{curl}\, \widetilde{S}_h^n(K)$. Hence, there exists $\varphi_h \in \widetilde{S}_h^n(K)$ such that $\mathbf{curl}\, \varphi_h = \beta_h \mathbf{v}_h$. In particular, we can use (3.29) to express φ_h as

$$\varphi_h(\mathbf{x}) = (R_{-\frac{\pi}{2}} \beta_h \mathbf{v}_h) \cdot (\mathbf{x} - \mathbf{x}^m) + c_0, \tag{3.46}$$

where $R_{-\frac{\pi}{2}}$ is the counterclockwise $\frac{\pi}{2}$ rotation matrix, and c_0 can be taken as an arbitrary constant with respect to which the projected vector is invariant. Then, for $\mathbf{u}_h \in \mathbf{V}_h^e$, it follows from integration by parts that

$$\int_K \beta_h \mathbf{\Pi}_K^{\beta_h} \mathbf{u}_h \cdot \mathbf{v}_h \, \mathrm{d}\mathbf{x} = \int_K \mathbf{u}_h \cdot \mathbf{curl}\, \varphi_h \, \mathrm{d}\mathbf{x} = \int_K \mathrm{curl}\ \mathbf{u}_h \, \varphi_h \, \mathrm{d}\mathbf{x} - \int_{\partial K} \mathbf{u}_h \cdot \mathbf{t} \, \varphi_h \, \mathrm{d}s, \tag{3.47}$$

where curl $\mathbf{u}_h$ is computable through DoFs as shown in (3.12). Notice that as $[\mathbf{u}_h \cdot \bar{\mathbf{t}}] = 0$ and φ_h is continuous on Γ_h^K, there is no contribution from the integral on Γ_h^K.

The projection for the $\mathbf{H}(\mathrm{div})$ case is defined similarly. A weighted L^2 projection is introduced $\widetilde{\mathbf{\Pi}}_K^{\beta_h^{-1}} : \mathbf{V}_h^f(K) \to \mathrm{curl}\, \widetilde{S}_h^n(K)$:

$$(\beta_h^{-1} \widetilde{\mathbf{\Pi}}_K^{\beta_h^{-1}} \mathbf{u}_h, \mathbf{v}_h)_K = (\beta_h^{-1} \mathbf{u}_h, \mathbf{v}_h)_K, \quad \forall \mathbf{v}_h \in \mathrm{curl}\, \widetilde{S}_h^n(K). \tag{3.48}$$

Given $\mathbf{v}_h \in \mathrm{curl}\, \widetilde{S}_h^n(K)$, there exists $\varphi_h \in S_h^n(K)$ such that $\nabla \varphi_h = \beta_h^{-1} \mathbf{v}_h$.

$$\int_K \beta_h^{-1} \mathbf{\Pi}_K^{\beta_h^{-1}} \mathbf{u}_h \cdot \mathbf{v}_h \, \mathrm{d}\mathbf{x} = \int_K \mathbf{u}_h \cdot \nabla \varphi_h \, \mathrm{d}\mathbf{x} = -\int_K \mathrm{div}\ \mathbf{u}_h \, \varphi_h \, \mathrm{d}\mathbf{x} + \int_{\partial K} \mathbf{u}_h \cdot \mathbf{n} \, \varphi_h \, \mathrm{d}s, \tag{3.49}$$

where div $\mathbf{u}_h$ can be computed through (3.16) with DoFs and $\mathbf{u}_h \cdot \mathbf{n}$ are the given DoFs.

In the rest of this article, for the sake of simplicity, we shall drop β_h of the projections $\Pi_K^{\beta_h}$ and $\mathbf{\Pi}_K^{\beta_h}$, and furthermore Π_K and $\mathbf{\Pi}_K$, regardless of being interface element or not, are adopted to maintain a consistent and concise set of notation. On each non-interface element, the projection is simply the identity operator.

4 Properties of IFE Functions

In this section, we recall some properties for IFE functions and show some novel ones to be used. In the following discussion, any subdomain $D \subseteq \Omega$, we denote for simplicity

$$\|u\|_{E,k,D} := \|u_E^+\|_{k,D} + \|u_E^-\|_{k,D} \quad \text{and} \quad \|\mathbf{u}\|_{E,\mathrm{curl},k,D} := \|\mathbf{u}\|_{E,k,D} + \|\operatorname{curl}\mathbf{u}\|_{E,k,D},$$

where k is a non-negative constant, and $u_E^{\pm}$ are the Sobolev extensions defined before Theorem 2.1. For scalar- or vector-valued functions, their corresponding seminorms adopt this notation convention as well. We also need the patch of an interface element K which is the collection of elements neighboring K:

$$\omega_K := \bigcup_{T\in\mathcal{T}_h,\overline{K}\cap\overline{T}\neq\emptyset} T, \quad \text{and} \quad \omega_K^{\pm} := \omega_K \cap \Omega^{\pm}.$$

In the following discussion, we focus our analysis on interface element where the specially constructed IVE and IFE spaces are used. The analysis on non-interface elements are trivial since the standard FE functions are used.

4.1 The H^1 IFE Functions

We first recall the trace inequalities for the H^1 IFE functions.

Lemma 11 (A trace inequality for H^1 IFE functions [53]) *For each interface element K and its edge e, there holds*

$$h_K^{1/2}\|\nabla v_h\|_{0,e} \lesssim \|\nabla v_h\|_{0,K}, \qquad \forall v_h \in S_h^n(K), \tag{4.1}$$

where the constant hidden in $\lesssim$ is independent of the location of the interface.

Result (4.1) is non-trivial in the sense that the hidden constant may depend on the interface location if classic tools are applied on each subelement. In particular, the constant may blow up when the cut subelement is degenerated. We refer readers to [53, Section 3.1] for a detailed proof. Heuristically for IFE functions, ∇v_h is a piecewise constant, and (4.1) is possible through scaling arguments. For IVE function v_h, however, such trace result may not be easy to establish as ∇v_h is non-polynomial in general and extra geometric conditions are needed, cf. [16]. This is also the case for the $\mathbf{H}(\mathrm{curl})$ IFE functions given in Lemma 18.

Let us then discuss the approximation results for the projection Π_K defined by (3.43). Similar to the standard H^1 projection, with the known approximation results for IFE interpolations in the literature [28, 32], the results for Π_K may directly follow from the best approximation property of the projection. However, we shall see that the analysis further demands the approximation of each polynomial component of $\Pi_K u$ on the whole element K. Recall that $\Pi_K u$ is piecewise linear in $K^{\pm}$ satisfying the jump condition (3.26). With a slight abuse of notation, we consider the two polynomial extensions of $\Pi_K u|_{K^{\pm}}$ defined on the entire element K

$$\Pi_K^{\pm} u := (\Pi_K u)_E^{\pm}, \tag{4.2}$$

where $(\Pi_K u)_E^{\pm}$ are trivial extensions of $\Pi_K u|_{K^{\pm}}$. Namely, we need to estimate $u_E^{\pm} - \Pi_K^{\pm} u$ on the entire element. See Fig. 3c for an illustration.

For this purpose, we need to employ a quasi-interpolation operator introduced in [32] as an intermediate tool which is denoted by $J_K u$. But, since our IFE functions are defined

with approximate interface Γ_h, we need to slightly modify the definition here. Define the interpolation operator J_K such that

$$J_K u = \begin{cases} J_K^+ u, & \text{in } \omega_K^+, \\ J_K^- u, & \text{in } \omega_K^-, \end{cases} \tag{4.3}$$

where $J_K^{\pm} u$ are two linear polynomials satisfying the following conditions

$$J_K^- u|_{\Gamma_h^K} = J_K^+ u|_{\Gamma_h^K} := \pi_{\omega_K} u_E^+|_{\Gamma_h^K}, \tag{4.4a}$$

$$\beta_h^- \nabla J_K^- u \cdot \bar{\mathbf{n}}_K = \beta_h^+ \nabla J_K^+ u \cdot \bar{\mathbf{n}}_K := \beta^- \nabla \pi_{\omega_K} u_E^-, \tag{4.4b}$$

where π_{ω_K} is the standard L^2 projection onto $\mathbb{P}_1(\omega_K)$. We note that the only difference between J_K and the one in [32] (denoted by I_T in (3.4) therein) is that the jump conditions are imposed on Γ_h^K.

Similar to (4.2), we denote the two polynomials that are trivial H^2-extensions of $J_K u|_{K^{\pm}}$ still as $J_K^{\pm} u$, which are defined on the whole element K. Roughly speaking, (4.4) defines a piecewise linear polynomial $J_K u$ by a Hermite interpolation at a point on Γ_h. Moreover, by an averaging type Taylor expansion, these two polynomials have the desired optimal approximations to their corresponding functions $u_E^{\pm}$ on the whole element. This crucial property is given by the lemma below, and serves as the key in our analysis.

Lemma 12 *For $u \in H^2(\beta; \mathcal{T}_h)$, on any $K \in \mathcal{T}_h^i$ there holds*

$$|u_E^{\pm} - J_K^{\pm} u|_{1,K} \lesssim h_K \|u\|_{E,2,\omega_K}. \tag{4.5}$$

Proof The argument is the same as Lemmas 3-5 in [32]. □

A similar estimate for $\Pi_K^{\pm}$ can be established on the whole element K. The analysis needs to employ the quasi interpolation $J_K^{\pm} u$ as an intermediate quantity to bridge the estimate.

Lemma 13 *For $u \in H^2(\beta; \mathcal{T}_h)$, on any $K \in \mathcal{T}_h^i$ there holds*

$$|u_E^{\pm} - \Pi_K^{\pm} u|_{1,K} \lesssim h_K \|u\|_{E,2,\omega_K} + |u|_{E,1,\delta K}. \tag{4.6}$$

Proof By the triangle inequality and Lemma 12, it suffices to estimate the difference $|J_K^{\pm} u^{\pm} - \Pi_K^{\pm} u|_{1,K}$. Without loss of generality, we only discuss the $+$ piece. We have the following trivial split

$$|J_K^+ u - \Pi_K^+ u|_{1,K} \lesssim \underbrace{|J_K^+ u - \Pi_K^+ u|_{1,K_h^+}}_{\text{(I)}} + \underbrace{|J_K^+ u - \Pi_K^+ u|_{1,K_h^-}}_{\text{(II)}}. \tag{4.7}$$

The estimate for (I) is relatively easy as the domain K_h^+ matches the definition of Π_K^+. By the triangle inequality,

$$\begin{aligned} |J_K^+ u - \Pi_K^+ u|_{1,K_h^+} &\lesssim |u - \Pi_K^+ u|_{1,K_h^+} + |u - J_K^+ u|_{1,K_h^+} \\ &\lesssim |u - \Pi_K u|_{1,K} + |u - J_K u|_{1,K} \\ &\lesssim |u - J_K u|_{1,K} \lesssim |u_E^{\pm} - J_K^{\pm} u|_{1,K} + |u|_{E,1,\delta K} \end{aligned} \tag{4.8}$$

where in the third inequality we have used the best approximation property for Π_K under the energy norm which is equivalent to the $|\cdot|_{1,K}$ norm.

The second term (II) is to estimate the error when the domain K_h^- is out of the part defining Π_K^+. Again we refer to Fig. 3c for an illustration. By the jump conditions on Γ_h^K and

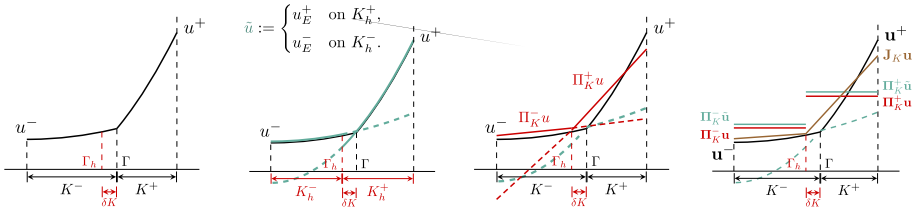

Fig. 3 A 1D analog of the comparison used in Lemmas 13 and 16: **a** and **b**: u and $\tilde{u} := u_E^{\pm}$ on $K_h^{\pm}$; **c**: $\Pi_K^{\pm} u$ for H^1 function in Lemma 13; **d**: $\Pi_K^{\pm}\mathbf{u}$ versus $\Pi_K^{\pm}\tilde{\mathbf{u}}$ for $\mathbf{H}(\mathrm{curl})$ case, where scalar functions in this figure is illustrated as the lateral view of the tangential component of the vector functions

employing the matrix in (3.28), we have the following identity for gradients of an IFE function $v_h \in S_h^n(K)$: $\nabla v_h^+ = M\nabla v_h^-$ with M given in (3.28). It clearly shows $\|\nabla v_h^+\| \simeq \|\nabla v_h^-\|$, where $\|\cdot\|$ are just Euclidean norms for vectors, and the hidden constant depends on β through the eigenvalues of M. Therefore, by letting $v_h = J_K u - \Pi_K u$, we have

$$|J_K^+ u - \Pi_K^+ u|_{1,K_h^-} \lesssim |J_K^- u - \Pi_K^- u|_{1,K_h^-} \tag{4.9}$$

where the later one can be proved similarly to (4.8). □

4.2 The H(curl) IFE Functions

The similar situation also exists for the $\mathbf{H}(\mathrm{curl})$ case, i.e., we need the estimates for the two polynomial components of the weighted L^2 projection $\mathbf{\Pi}_K^{\pm}\mathbf{u}$ on the entire element (the notation is similar to (4.2)). In this case, we employ the quasi interpolation defined in [31, (4.4)] as an intermediate estimate in the error analysis, which is similar to that for (4.3). Here we denote it as $\mathbf{J}_K$ to be distinguished from the H^1 scalar case of which the approximation is recalled below:

Lemma 14 (Theorem 4.1 in [31]) *For $\mathbf{u} \in \mathbf{H}^1(\mathrm{curl}, \alpha, \beta; \mathcal{T}_h)$, on any $K \in \mathcal{T}_h^i$ there holds*

$$\|\mathbf{u}_E^{\pm} - \mathbf{J}_K^{\pm}\mathbf{u}\|_{\mathbf{H}(\mathrm{curl};K)} \lesssim h_K \|\mathbf{u}\|_{E,\mathrm{curl},1,\omega_K}. \tag{4.10}$$

We also recall the following result.

Lemma 15 (Lemma 4.2 in [31] and Lemma 5.4 in [12]) *For $\mathbf{u} \in \mathbf{H}^1(\mathrm{curl}, \alpha, \beta; \mathcal{T}_h)$, on any $K \in \mathcal{T}_h^i$, the difference of the extensions on the approximate interface Γ_h^K along the tangential direction $\bar{\mathbf{t}}$ satisfies*

$$\|\mathbf{u}_E^+ \cdot \bar{\mathbf{t}} - \mathbf{u}_E^- \cdot \bar{\mathbf{t}}\|_{0,K} \lesssim h_K \|\mathbf{u}\|_{E,1,\omega_K}. \tag{4.11}$$

As a function in $\mathbf{H}(\mathrm{curl})$, $\mathbf{u}\cdot\mathbf{t}$ is continuous. Extension will preserve the tangential continuity. Note that $\mathbf{u}_E^+ \cdot \mathbf{t} = \mathbf{u}_E^- \cdot \mathbf{t}$ on $\Gamma \cap K$, then it is reasonable to expect $\mathbf{u}_E^+ \cdot \bar{\mathbf{t}}$ is close to $\mathbf{u}_E^- \cdot \bar{\mathbf{t}}$ on Γ_h^K as $\bar{\mathbf{t}}$ is a good approximation to $\mathbf{t}$. As both the two quantities $\mathbf{u}_E^{\pm} \cdot \bar{\mathbf{t}}$ are well-defined on the entire element K, the estimate in (4.11) is a Poincaré-type inequality in a certain sense.

Then we can show the estimates for $\mathbf{\Pi}_K\mathbf{u}$ and curl $\mathbf{u}_I$. For the curl case, we need to eliminate the mismatch term on δK in the error bound. For this purpose, we note that the mismatched term is essentially caused by the fact that $\mathbf{u}$ itself is partitioned by Γ but $\mathbf{\Pi}_K\mathbf{u}$ and $\mathbf{u}_I$ are partitioned by Γ_h. So, it inspires us to introduce a new function $\tilde{\mathbf{u}} := \mathbf{u}_E^{\pm}$ on $K_h^{\pm}$

as an intermediate quantity, and present the following estimate. Note that $\tilde{\mathbf{u}} = \mathbf{u}$ on ∂K, and thus $\tilde{\mathbf{u}}_I = \mathbf{u}_I$. In fact, $\tilde{\mathbf{u}}$ differs from $\mathbf{u}$ only on the mismatched region δK, i.e., on $\delta K \cap K_h^+$, $\mathbf{u} - \tilde{\mathbf{u}} = \mathbf{u} - \mathbf{u}_E^+ = \mathbf{u}_E^- - \mathbf{u}_E^+$, and similarly on $\delta K \cap K_h^-$, $\mathbf{u} - \tilde{\mathbf{u}} = \mathbf{u}_E^+ - \mathbf{u}_E^-$. We also note that $[\tilde{\mathbf{u}} \cdot \bar{\mathbf{t}}]\,|_{\Gamma_h^K} \neq 0$. For an analog of this heuristic in a 1-dimensional setting, please refer to Fig. 3d.

Lemma 16 *Let* $\tilde{\mathbf{u}} := \mathbf{u}_E^{\pm}$ *on* $K_h^{\pm}$, *then there holds*

$$\|\mathbf{\Pi}_K^{\pm}\mathbf{u} - \mathbf{\Pi}_K^{\pm}\tilde{\mathbf{u}}\|_{0,K} \lesssim h_K \|\mathbf{u}\|_{E,\mathrm{curl},1,\omega_K}, \tag{4.12a}$$

$$\mathrm{curl}\ \mathbf{u}_I = \mathrm{curl}\ \tilde{\mathbf{u}}_I. \tag{4.12b}$$

Proof Since $\mathbf{u}$ and $\tilde{\mathbf{u}}$ match on ∂K, (4.12b) is trivial from integration by parts. We estimate $\mathbf{\Pi}_K\mathbf{u} - \mathbf{\Pi}_K\tilde{\mathbf{u}} := \mathbf{w}_h$. Given each $\mathbf{v}_h \in \nabla S_h^n(K)$, by (3.41), we can find $\varphi_h \in \widetilde{S}_h^n(K)$ satisfying $\mathbf{curl}\,\varphi_h = \beta_h \mathbf{v}_h$ given in Remark 5. For $\mathbf{v} = \mathbf{u}$ or $\tilde{\mathbf{u}}$, a similar formula to (3.47) leads to

$$\int_K \beta_h \mathbf{\Pi}_K\mathbf{v} \cdot \mathbf{v}_h \,\mathrm{d}\mathbf{x} = \int_K \mathrm{curl}\ \mathbf{v}\, \varphi_h \,\mathrm{d}\mathbf{x} - \int_{\partial K} \mathbf{v} \cdot \bar{\mathbf{t}} \varphi_h \,\mathrm{d}s - \int_{\Gamma_h^K} [\mathbf{v} \cdot \bar{\mathbf{t}}]\varphi_h \,\mathrm{d}s \tag{4.13}$$

where the last term vanishes for $\mathbf{v} = \mathbf{u}$. Using the fact that $\mathbf{u}$ and $\tilde{\mathbf{u}}$ match on ∂K and taking the difference of (4.13) for $\mathbf{v} = \mathbf{u}$ and $\tilde{\mathbf{u}}$, we have

$$\int_K \beta_h \mathbf{w}_h \cdot \mathbf{v}_h \,\mathrm{d}\mathbf{x} = \underbrace{\int_{\delta K} \mathrm{curl}\,(\mathbf{u} - \tilde{\mathbf{u}})\, \varphi_h \,\mathrm{d}\mathbf{x}}_{\text{(I)}} - \underbrace{\int_{\Gamma_h^K} (\mathbf{u}_E^+ \cdot \bar{\mathbf{t}} - \mathbf{u}_E^- \cdot \bar{\mathbf{t}})\varphi_h \,\mathrm{d}s}_{\text{(II)}}. \tag{4.14}$$

By Hölder's inequality and (3.42), we have

$$\text{(I)} \lesssim \|\,\mathrm{curl}\,(\mathbf{u}_E^+ - \mathbf{u}_E^-)\|_{0,\delta K} \|\varphi_h\|_{0,K} \lesssim h_K \|\,\mathrm{curl}\,(\mathbf{u}_E^+ - \mathbf{u}_E^-)\|_{0,\delta K} \|\mathbf{v}_h\|_{0,K}. \tag{4.15}$$

Using the trace inequality in Lemma 4, (3.42), and $\mathbf{curl}\,\varphi_h = \beta_h \mathbf{v}_h$ yields

$$\begin{aligned} \text{(II)} &\lesssim (h_K^{-1/2}\|\mathbf{u}_E^+ \cdot \bar{\mathbf{t}} - \mathbf{u}_E^- \cdot \bar{\mathbf{t}}\|_{0,K} + h_K^{1/2}|\mathbf{u}_E^+ \cdot \bar{\mathbf{t}} - \mathbf{u}_E^- \cdot \bar{\mathbf{t}}|_{1,K}) \cdot (h_K^{-1/2}\|\varphi_h\|_{0,K} + h_K^{1/2}|\varphi_h|_{1,K}) \\ &\lesssim \|\mathbf{u}_E^+ \cdot \bar{\mathbf{t}} - \mathbf{u}_E^- \cdot \bar{\mathbf{t}}\|_{0,K} \|\mathbf{v}_h\|_{0,K} + h_K |\mathbf{u}_E^+ \cdot \bar{\mathbf{t}} - \mathbf{u}_E^- \cdot \bar{\mathbf{t}}|_{1,K} \|\mathbf{v}_h\|_{0,K} \\ &\lesssim h_K \|\mathbf{u}\|_{E,1,\omega_K} \|\mathbf{v}_h\|_{0,K} \end{aligned} \tag{4.16}$$

where we have used Lemma 15 in the third inequality. Putting (4.15) and (4.16) into (4.14), letting $\mathbf{v}_h = \mathbf{w}_h$, and cancelling one $\|\mathbf{w}_h\|_{0,K}$ on each side, we obtain

$$\|\mathbf{\Pi}_K\mathbf{u} - \mathbf{\Pi}_K\tilde{\mathbf{u}}\|_{0,K} \lesssim h_K(\|\,\mathrm{curl}\,(\mathbf{u}_E^+ - \mathbf{u}_E^-)\|_{0,\delta K} + \|\mathbf{u}\|_{E,1,\omega_K}). \tag{4.17}$$

Note that $\mathbf{\Pi}_K\mathbf{u} - \mathbf{\Pi}_K\tilde{\mathbf{u}} \in \nabla S_h^n(K)$ by the exact sequence. So, using the argument similar to (4.9), we directly induce (4.12a) from (4.17). □

With this preparation, we will present the following crucial estimate.

Lemma 17 *For* $\mathbf{u} \in \mathbf{H}^1(\mathrm{curl}, \alpha, \beta; \mathcal{T}_h)$, *on any* $K \in \mathcal{T}_h^i$ *there holds*

$$\|\mathbf{\Pi}_K^{\pm}\mathbf{u} - \mathbf{u}_E^{\pm}\|_{0,K} \lesssim h_K \|\mathbf{u}\|_{E,\mathrm{curl},1,\omega_K}, \tag{4.18a}$$

$$\|\,\mathrm{curl}\ \mathbf{u}_E^{\pm} - \mathrm{curl}^{\pm}\mathbf{u}_I\|_{0,K} \lesssim h_K \|\mathbf{u}\|_{E,\mathrm{curl},1,\omega_K}, \tag{4.18b}$$

where $\mathrm{curl}^{\pm}\mathbf{u}_I = (\mathrm{curl}\ \mathbf{u}_I)^{\pm}$ *are the two constants used on the whole element.*

Proof The argument is similar to Lemma 13 but slightly more complicated, since we need to avoid the mismatched region δK by employing the function $\tilde{\mathbf{u}}$ introduced in Lemma 16. We decompose the argument into several steps.

Step 1. We show

$$\|\tilde{\mathbf{u}} - \mathbf{\Pi}_K \tilde{\mathbf{u}}\|_{0,K} \lesssim h_K \|\mathbf{u}\|_{E,\mathrm{curl},1,\omega_K}. \tag{4.19}$$

Thanks to (3.33), we can write $\mathbf{J}_K\mathbf{u}$ as

$$\mathbf{J}_K\mathbf{u} = \mathbf{p} + p_0(-(x_2 - x_2^m), x_1 - x_1^m)^\intercal, \tag{4.20}$$

where p_0 and $\mathbf{p}$ are piecewise scalar- and vector-valued constants. In particular, we have $\mathbf{p} \in \nabla S_h(K) = \mathrm{Ker}(\mathrm{curl}) \cap \mathbf{S}_h^e(K)$, and $p_0 = \mathrm{curl}\ \mathbf{J}_K\mathbf{u}/2$. Then, by the best approximation property of the projection, we have

$$\begin{aligned} \|\tilde{\mathbf{u}} - \mathbf{\Pi}_K \tilde{\mathbf{u}}\|_{0,K} &\lesssim \|\sqrt{\beta_h}(\tilde{\mathbf{u}} - \mathbf{\Pi}_K \tilde{\mathbf{u}})\|_{0,K} \lesssim \|\sqrt{\beta_h}(\tilde{\mathbf{u}} - \mathbf{p})\|_{0,K} \\ &\lesssim \|\tilde{\mathbf{u}} - \mathbf{J}_K\mathbf{u}\|_{0,K} + h_K \|\mathrm{curl}\ \mathbf{J}_K\mathbf{u}\|_{0,K}, \end{aligned} \tag{4.21}$$

where in the last inequality we have inserted $p_0(x_2 - x_2^m, -(x_1 - x_1^m))^\intercal$. Noticing that the partition of $\tilde{\mathbf{u}}$ exactly matches $\mathbf{J}_K\mathbf{u}$, i.e., both of their piecewise definitions are separated by Γ_h^K. Hence, applying Lemma 14 yields (4.19).

Step 2. We refine the estimate in (4.19) to the entire element; namely, with $\tilde{\mathbf{u}}^\pm = \mathbf{u}_E^\pm$, we need to show

$$\|\mathbf{u}_E^\pm - \mathbf{\Pi}_K^\pm \tilde{\mathbf{u}}\|_{0,K} \lesssim h_K \|\mathbf{u}\|_{E,\mathrm{curl},1,\omega_K}. \tag{4.22}$$

Without loss of generality, we focus on $\mathbf{\Pi}_K^+\tilde{\mathbf{u}} - \mathbf{u}_E^+$. Similar to the argument in Lemma 13, we only need to estimate $\|\mathbf{\Pi}_K^+\tilde{\mathbf{u}} - \mathbf{J}_K^+\mathbf{u}\|_{0,K_h^-}$. Again, let us write

$$\mathbf{\Pi}_K^+\tilde{\mathbf{u}} - \mathbf{J}_K^+\mathbf{u} = \mathbf{q} + q_0(x_2 - x_2^m, -(x_1 - x_1^m))^\intercal, \tag{4.23}$$

where q_0 and $\mathbf{q}$ are piecewise scalar- and vector-valued constants. Next, we notice $\mathbf{q}^+ = M\mathbf{q}^-$ and $\alpha^+ q_0^+ = \alpha^- q_0^-$. Then, we have

$$\begin{aligned} \|\mathbf{\Pi}_K^+\tilde{\mathbf{u}} - \mathbf{J}_K^+\mathbf{u}\|_{0,K_h^-} &\lesssim \|\mathbf{q}^+\|_{0,K_h^-} + h_K\|q_0^+\|_{0,K_h^-} \lesssim \|M\mathbf{q}^-\|_{0,K_h^-} + h_K\|q_0^-\|_{0,K_h^-} \\ &\lesssim \|\mathbf{\Pi}_K^-\mathbf{u} - \mathbf{J}_K^-\mathbf{u}\|_{0,K_h^-} + h_K\|\mathrm{curl}(\mathbf{\Pi}_K^-\mathbf{u} - \mathbf{J}_K^-\mathbf{u})\|_{0,K_h^-}, \end{aligned} \tag{4.24}$$

where in the last inequality we have inserted $q_0^-(-(x_2 - x_2^m), x_1 - x_1^m)^\intercal$ and used $q_0 = \mathrm{curl}(\mathbf{\Pi}_K\tilde{\mathbf{u}} - \mathbf{J}_K\mathbf{u})$. Now, inserting $\tilde{\mathbf{u}}^- = \mathbf{u}_E^-$ in the right-hand side of (4.24), applying Lemma 14, and (4.19) in Step 1 lead to the desired estimate (4.22) of Step 2. This wraps up the case of $+$. Combing (4.12a) and (4.22) through the triangle inequality finishes the proof of (4.18a).

Step 3. As for (4.18b), by Lemma 9 and (4.12b), we use that the projections are the best approximation to obtain

$$\|\sqrt{\alpha_h}(\mathrm{curl}\ \tilde{\mathbf{u}} - \mathrm{curl}\ \mathbf{u}_I)\|_{0,K} \le \|\sqrt{\alpha_h}(\mathrm{curl}\ \tilde{\mathbf{u}} - \mathrm{curl}\,\mathbf{J}_K\mathbf{u})\|_{0,K} \lesssim h_K\|\mathbf{u}\|_{E,\mathrm{curl},1,\omega_K}, \tag{4.25}$$

where we have also applied Lemma 14. Again, we have taken the advantage that both $\tilde{\mathbf{u}}$ and $\mathbf{J}_K\mathbf{u}$ are piecewisely defined on K separated by Γ_h^K. Then, similar to the argument above, it only remains to estimate

$$\|\mathrm{curl}\,(\mathbf{J}_K^+\mathbf{u} - \mathbf{u}_I^+)\|_{0,K_h^-} \le \frac{\alpha_h^-}{\alpha_h^+}\|\mathrm{curl}\,(\mathbf{J}_K^-\mathbf{u} - \mathbf{u}_I^-)\|_{0,K_h^-}.$$

The right hand side above follows from inserting curl $\mathbf{u}_E^-$ in between, and applying (4.25) and Lemma 14 respectively on the two terms from the triangle inequality. □

Finally, the trace inequality also holds for $\mathbf{H}(\text{curl})$ IFE functions regardless of interface location.

Lemma 18 (A trace inequality for $\mathbf{H}(\text{curl})$ IFE functions [31]) *For each interface element K and its edge e, there holds*

$$\|\mathbf{v}_h\|_{0,e} \lesssim h_K^{-1/2}\|\mathbf{v}_h\|_{0,K}, \qquad \forall \mathbf{v}_h \in \mathbf{S}_h^e(K). \tag{4.26}$$

5 H^1 Elliptic Interface Problems

In this section, we present the IVE method for solving the H^1-elliptic interface problem and give the optimal order convergence analysis.

5.1 Scheme

Define the local bilinear form on an interface element K as: $a_h^{n,K}(\cdot,\cdot) : H^1(K) \times H^1(K) \to \mathbb{R}$ where

$$a_h^{n,K}(u_h, v_h) := (\beta_h \nabla \Pi_K u_h, \nabla \Pi_K v_h)_K + S_K^n(u_h - \Pi_K u_h, v_h - \Pi_K v_h). \tag{5.1}$$

One of the keys for VEM is the choice of the stabilization term. Here, following [10], we consider the one associated with the $H^{1/2}(e)$ seminorm on $e \in \mathcal{E}_K$:

$$(w_h, z_h)_{1/2,e} := \int_e \int_e \beta_e \frac{(w_h(\mathbf{x}) - w_h(\mathbf{y}))(z_h(\mathbf{x}) - z_h(\mathbf{y}))}{|\mathbf{x} - \mathbf{y}|^2} \, \mathrm{d}s(\mathbf{x}) \, \mathrm{d}s(\mathbf{y}), \tag{5.2}$$

where $\beta_e = \beta_h|_e$. Accordingly, $|\cdot|_{1/2,\mathcal{E}_K}$ is defined for any $w \in \Pi_{e\in\mathcal{E}_K} H^{1/2}(e)$ as

$$|w|_{1/2,\mathcal{E}_K}^2 := \sum_{e\in\mathcal{E}_K} (w, w)_{1/2,e}. \tag{5.3}$$

Then, the stabilization term $S_K^n(\cdot,\cdot)$ is

$$S_K^n(w_h, z_h) := \sum_{e\in\mathcal{E}_K} \beta_e (w_h, z_h)_{1/2,e} = \sum_{e\in\mathcal{E}_K} \beta_e (w_h(\mathbf{b}_e) - w_h(\mathbf{a}_e))(z_h(\mathbf{b}_e) - z_h(\mathbf{a}_e)). \tag{5.4}$$

where the second identity is due to that both w_h and z_h are linear functions on each $e \in \mathcal{E}_K$. The difference-type stabilization in (5.4) is first proposed in [73], and then analyzed in [68]. Here we choose the discrete $1/2$ inner product as the error analysis is robust to the edge length. For example, short edges are indeed unavoidable in our setting, of which the presence does not affect the robustness of the analysis. The proposed IVE scheme for solving (1.1) is to find $u_h \in V_h^n$ such that

$$a_h^n(u_h, v_h) := \sum_{K\in\mathcal{T}_h} a_h^{n,K}(u_h, v_h) = \sum_{K\in\mathcal{T}_h} (f, \Pi_K v_h)_K, \quad \forall v_h \in V_h^n, \tag{5.5}$$

where the bilinear form on non-interface elements is simply the standard one $(\beta_h \nabla u_h, \nabla v_h)_K$. The well-posedness of the scheme above is given by Lemma 19 below. We define the energy norm

$$|||v_h|||_n^2 := a_h^n(v_h, v_h). \tag{5.6}$$

Lemma 19 *$|||\cdot|||_n$ is a norm on $H_0^1(\Omega) \cap V_h^n$.*

Proof Suppose $|||v_h|||_n = 0$ for some $v_h \in H_0^1(\Omega) \cap V_h^n$. on any $K \in \mathcal{T}_h^i$, by (5.1), $\|\beta_h^{1/2} \nabla \Pi_K v_h\|_{0,K} = 0$ implies $\Pi_K v_h \in \mathbb{P}_0(K)$. Moreover, $|(\mathrm{I} - \Pi_K)v_h|_{1/2,e} = 0$ implies $v_h \in \mathbb{P}_0(e)$ on each $e \in \mathcal{E}_K$. By $v_h \in C^0(\partial K) \cap H^1(K)$ in (3.1), $v_h \in \mathbb{P}_0(K)$. The same result holds on non-interface elements trivially. Therefore, the continuity in (3.2) and the boundary condition on $\partial\Omega$ lead to $v_h \equiv 0$. □

5.2 An Error Equation

Given $u \in H^2(\beta, \mathcal{T}_h)$, since the global virtual element space V_h^n is conforming, there always holds $u_I \in H^1(\Omega)$ given by (3.25). Our analysis is based on the following error decomposition:

$$\xi_h = u - u_I \qquad \text{and} \qquad \eta_h = u_I - u_h. \tag{5.7}$$

The estimate of ξ_h is from the interpolation error estimate and η_h will be derived from an error equation. The IVE and IFE coincide with the standard simplicial finite element consisting only polynomials, thus the proposed stabilization vanishes. As a result, estimates on non-interface elements fall into the standard FEM regime; and our focus will be thus on the interface elements.

We follow [10] to derive an error equation for $\eta_h = u_I - u_h$.

Lemma 20 (Error equation) *Let $u \in H^2(\beta; \mathcal{T}_h)$ be the solution to (1.1) and u_h be the solution to (5.5). Denote by $\eta_h = u_h - u_I$, then the following identity holds*

$$\begin{aligned} |||\eta_h|||_n^2 = \sum_{K\in\mathcal{T}_h} \Big\{ &(\beta_h \nabla \Pi_K (u - u_I), \nabla \Pi_K \eta_h)_K + (\beta_h \nabla (u - \Pi_K u) \cdot \mathbf{n}, \eta_h - \Pi_K \eta_h)_{\partial K} \\ &- S_K^n(u_I - \Pi_K u_I, \eta_h - \Pi_K \eta_h) + ((\beta - \beta_h)\nabla u, \nabla \Pi_K \eta_h)_K \Big\}. \end{aligned} \tag{5.8}$$

Proof We start by the following

$$\begin{aligned} |||\eta_h|||_n^2 &= a_h^n(u_h, \eta_h) - a_h^n(u_I, \eta_h) \\ &= \sum_{K\in\mathcal{T}_h} (f, \Pi_K \eta_h)_K - a_h^n(u_I, \eta_h) \quad \text{(Problem (5.5))} \\ &= \sum_{K\in\mathcal{T}_h} (-\nabla \cdot (\beta \nabla u), \Pi_K \eta_h)_K - a_h^n(u_I, \eta_h) \quad \text{(Original PDE)} \\ &= \sum_{K\in\mathcal{T}_h} \big[\underbrace{(\beta \nabla u, \nabla \Pi_K \eta_h)_K}_{\text{(I)}} - \underbrace{(\beta \nabla u \cdot \mathbf{n}, \Pi_K \eta_h)_{\partial K}}_{\text{(II)}} \big] - a_h^n(u_I, \eta_h). \quad \text{(Integration by parts)} \end{aligned} \tag{5.9}$$

In the last identity above, the flux jump conditions of u (1.2) and the continuity of $\Pi_K \eta_h$ on K are also used. For the term (I) in (5.9), using the definition of Π_K we have

$$\begin{aligned} \text{(I)} &= (\beta_h \nabla u, \nabla \Pi_K \eta_h)_K + ((\beta - \beta_h)\nabla u, \nabla \Pi_K \eta_h)_K \\ &= (\beta_h \nabla \Pi_K u, \nabla \Pi_K \eta_h)_K + ((\beta - \beta_h)\nabla u, \nabla \Pi_K \eta_h)_K. \end{aligned} \tag{5.10}$$

For the term (II), since $\beta = \beta_h$ on ∂K, we obtain

$$\sum_{K\in\mathcal{T}_h} (\mathrm{II}) = \sum_{K\in\mathcal{T}_h} (\beta_h \nabla u \cdot \mathbf{n}, \Pi_K \eta_h)_{\partial K} = \sum_{K\in\mathcal{T}_h} (\beta_h \nabla u \cdot \mathbf{n}, \Pi_K \eta_h - \eta_h)_{\partial K}, \tag{5.11}$$

where in the second identity we have used $\eta_h = u_h - u_I$ being continuous across each edge as it is in the virtual element space V_h^n. Using integration by parts on the subelements $K_h^{\pm}$, the flux jump conditions of the IFE functions on Γ_h^K, $\eta_h - \Pi_K \eta_h$ being continuous across Γ_h^K, and definition of the projection Π_K, we have

$$\begin{aligned}(\beta_h \nabla \Pi_K u \cdot \mathbf{n}, \eta_h - \Pi_K \eta_h)_{\partial K} &= \sum_{s=\pm} (\beta_h \nabla \Pi_K u \cdot \mathbf{n}, \eta_h - \Pi_K \eta_h)_{\partial K_h^s} \\ &= \sum_{s=\pm} (\beta_h \nabla \Pi_K u, \nabla(\eta_h - \Pi_K \eta_h))_{K_h^s} = 0.\end{aligned} \tag{5.12}$$

Thus, (5.11) further becomes

$$\sum_{K\in\mathcal{T}_h} (\mathrm{II}) = \sum_{K\in\mathcal{T}_h} (\beta_h \nabla (u - \Pi_K u) \cdot \mathbf{n}, \Pi_K \eta_h - \eta_h)_{\partial K}. \tag{5.13}$$

Putting (5.10) and (5.13) into (5.9), and using the formula of $a_h^n(u_I, v_h)$, we obtain the desired result. □

In the derivation above, there are two steps involving integration by parts: the one in (5.9) is for the exact solution u with respect to the subelements $K^{\pm}$, and another one in (5.12) is for IVE and IFE functions with respect to the subelements $K_h^{\pm}$. Their difference corresponds to their respective jump conditions imposed on Γ or Γ_h^K, such that those extra terms occurring on Γ or Γ_h^K can be cancelled.

5.3 Error Estimates

In this section, we proceed to estimate the solution errors. Based on the error equation in Lemma 20, we first get an error bound for $u_h - u_I$.

Theorem 5.1 (A priori error bound) *Let $u \in H^2(\beta; \mathcal{T}_h)$ be the solution to (1.1) and u_h be the solution to (5.5). Denote by $\eta_h = u_h - u_I$. Then there holds*

$$|||\eta_h|||_n \lesssim \sum_{K\in\mathcal{T}_h} \Big[\|\beta_h^{1/2} \nabla \Pi_K (u - u_I)\|_{0,K} + h_K^{1/2} \|\beta_h^{1/2} \nabla (u - \Pi_K u) \cdot \mathbf{n}\|_{0,\partial K} \tag{5.14}$$

$$+ |\beta_h^{1/2} (u_I - \Pi_K u_I)|_{1/2,\mathcal{E}_K} + \|\beta_{\max}^{1/2} \nabla u\|_{0,\delta K} \Big]. \tag{5.15}$$

Proof Note that $\beta \neq \beta_h$ only on δK, thus for the error equation in Lemma 20, applying the Cauchy-Schwarz inequality, we have

$$\begin{aligned}|||\eta_h|||_n^2 \leq \sum_{K\in\mathcal{T}_h} \Big(&\|\beta_h^{1/2} \nabla \Pi_K (u - u_I)\|_{0,K} \|\beta_h^{1/2} \nabla \Pi_K \eta_h\|_{0,K} \\ &+ \|\beta_h^{1/2} \nabla (u - \Pi_K u) \cdot \mathbf{n}\|_{0,\partial K} \|\beta_h^{1/2} (\eta_h - \Pi_K \eta_h)\|_{0,\partial K} \\ &+ |\beta_h^{1/2} (u_I - \Pi_K u_I)|_{1/2,\mathcal{E}_K} |\beta_h^{1/2} (\eta_h - \Pi_K \eta_h)|_{1/2,\mathcal{E}_K} \\ &+ \|\beta_{\max}^{1/2} \nabla u\|_{0,\delta K} \|\beta_{\max}^{1/2} \nabla \Pi_K \eta_h\|_{0,K} \Big).\end{aligned} \tag{5.16}$$

In the bound above, it is clear that $\|\beta_h^{1/2}\nabla\Pi_K\eta_h\|_{0,K}$ and $|\beta_h^{1/2}(\eta_h-\Pi_K\eta_h)|_{1/2,\mathcal{E}_K}$ are bounded above by $|||\eta_h|||_n$, and $\|\beta_{\max}^{1/2}\nabla\Pi_K\eta_h\|_{0,K}$ is also bounded above by $|||\eta_h|||_n$ with a β dependent constant.

To estimate the remaining second term in (5.16), we note that $\int_{\partial K}(\eta_h-\Pi_K\eta_h)\,\mathrm{d}s=0$, thus applying (2.8a) edge-wise in Theorem 2.2 yields

$$\|\beta_h^{1/2}(\eta_h-\Pi_K\eta_h)\|_{0,\partial K}\lesssim h_K^{1/2}|\beta_h^{1/2}(\eta_h-\Pi_K\eta_h)|_{1/2,\mathcal{E}_K}\lesssim h_K^{1/2}|||\eta_h|||_n.$$

Combining the estimates above and cancelling out a $|||\eta_h|||_n$ on each side, we get the desired a priori estimate. □

To get the optimal order of convergence of the proposed method, our task is to estimate each term on the right-hand side of the error bound (5.14). Before getting into the estimate, we emphasize that the set $\mathcal{E}_K$ consists of the edges formed by element vertices and cut points. Therefore, to avoid confusion in the following discussion, for each edge $e\in\mathcal{E}_K$ that connects an element vertex and a cut point, we will use $\hat{e}$ to denote the edge containing e on the triangle in the background mesh (e.g. $e=\overline{\mathbf{a}_1\mathbf{b}_1}$ to $\hat{e}=\overline{\mathbf{a}_1\mathbf{a}_2}$ in Fig. 2a). Now, let us first derive the estimate of the first term in the right-hand side of the error bound in (5.14).

Lemma 21 *Let $u\in H^2(\beta;\mathcal{T}_h)$, then on any $K\in\mathcal{T}_h^i$ there holds*

$$\|\beta_h^{1/2}\nabla\Pi_K(u-u_I)\|_{0,K}\lesssim h_K\|u\|_{E,2,\omega_K}. \tag{5.17}$$

Proof By the definition of projection, we immediately have

$$\begin{aligned}\|\beta_h^{1/2}\nabla\Pi_K(u-u_I)\|_{0,K}^2&=(\beta_h\nabla\Pi_K(u-u_I),\\ \nabla\Pi_K(u-u_I))_K&=(\beta_h\nabla\Pi_K(u-u_I),\nabla(u-u_I))_K.\end{aligned}$$

Using integration by parts on the subelements $K_h^{\pm}$, $\Pi_K(u-u_I)$ satisfying the jump condition on Γ_K, and $u-u_I\in H^1(K)$, we have

$$\begin{aligned}\|\beta_h^{1/2}\nabla\Pi_K(u-u_I)\|_{0,K}^2=&(\beta_h\nabla\Pi_K(u-u_I)\cdot\mathbf{n},u-u_I)_{\partial K}\\ \le&\|\beta_h^{1/2}\nabla\Pi_K(u-u_I)\cdot\mathbf{n}\|_{0,\partial K}\|\beta_h^{1/2}(u-u_I)\|_{0,\partial K}.\end{aligned} \tag{5.18}$$

For each edge on ∂K, applying the IFE trace inequality in Theorem 11, we obtain

$$\begin{aligned}\|\beta_h^{1/2}\nabla\Pi_K(u-u_I)\cdot\mathbf{n}\|_{0,e}&\le\|\beta_h^{1/2}\nabla\Pi_K(u-u_I)\cdot\mathbf{n}\|_{0,\hat{e}}\\ &\lesssim h_K^{-1/2}\|\beta_h^{1/2}\nabla\Pi_K(u-u_I)\|_{0,K}.\end{aligned} \tag{5.19}$$

Putting (5.19) into (5.18) and cancelling out the term $\|\beta_h^{1/2}\nabla\Pi_K(u-u_I)\|_{0,K}$ leads to

$$\|\beta_h^{1/2}\nabla\Pi_K(u-u_I)\|_{0,K}\lesssim h_K^{-1/2}\|\beta_h^{1/2}(u-u_I)\|_{0,\partial K}. \tag{5.20}$$

So it remains to estimate the right-hand side above. Notice β_h is constant on each edge $e\in\mathcal{E}_K$. Without loss of generality, consider an $e\subset\partial K^+$, by the interpolation estimate on this edge, we have

$$\|\beta_h^{1/2}(u-u_I)\|_{0,e}\lesssim h_e^{3/2}|u|_{3/2,e}\lesssim h_K^{3/2}|u_E^+|_{3/2,\hat{e}}\lesssim h_K^{3/2}|u_E^+|_{2,K} \tag{5.21}$$

where in the last inequality, we have also applied the trace inequality in [10, Lemma 6.2] on $\nabla u_E^+|_{\hat{e}}$. Putting (5.21) into (5.20) gives the desired estimate on this edge. Similar arguments apply to the case $e\subset\partial K^-$ which together finishes the proof. □

The estimate of the second and third terms in the right-hand side of the error bound (5.14) relies on the estimate of every polynomial component of $\Pi_K^{\pm}$ on the whole element K which has been established in Lemma 13.

Lemma 22 *Let $u \in H^2(\beta; \mathcal{T}_h)$, then on any $K \in \mathcal{T}_h^i$ there holds*

$$\|\beta_h^{1/2}\nabla(u - \Pi_K u)\cdot\mathbf{n}\|_{0,\partial K} \lesssim h_K^{1/2}\|u\|_{E,2,\omega_K} + h_K^{-1/2}|u|_{E,1,\delta K}. \tag{5.22}$$

Proof Without loss of generality, we only consider $+$ side. Given an edge $e \in \mathcal{E}_K$ with $e \subseteq K_h^+$ and its extension $\hat{e}$ as an edge of K, we apply the trace inequality to obtain

$$\begin{aligned}\|\beta_h\nabla(u - \Pi_K u)\cdot\mathbf{n}\|_{0,e} &\le (\beta^+)^{1/2}\|\nabla(u_E^+ - \Pi_K^+ u)\cdot\mathbf{n}\|_{0,\hat{e}}\\ &\lesssim h_K^{-1/2}|u_E^+ - \Pi_K^+ u|_{1,K} + h_K^{1/2}|u_E^+|_{2,K}\end{aligned}$$

which yields the desired result by Lemma 13. □

Lemma 23 *Let $u \in H^2(\beta; \mathcal{T}_h)$, then on any $K \in \mathcal{T}_h^i$ there holds*

$$|\beta_h^{1/2}(u_I - \Pi_K u_I)|_{1/2,\mathcal{E}_K} \lesssim h_K\|u\|_{E,2,\omega_K} + |u|_{E,1,\delta K}. \tag{5.23}$$

Proof Recall that $|\cdot|_{1/2,\mathcal{E}_K}$ is defined in (5.3). It suffices to establish an edge-wise estimate under $|\cdot|_{1/2,e}$ of which the definition is given in (5.2). For each edge, since β_h is a constant,

$$|\beta_h^{1/2}(u_I - \Pi_K u_I)|_{1/2,e} \lesssim \underbrace{|u_I - \Pi_K u|_{1/2,e}}_{\text{(I)}} + \underbrace{|\Pi_K(u - u_I)|_{1/2,e}}_{\text{(II)}}.$$

In the following discussion, without loss of generality we only consider $e \subseteq K_h^+$. For (I), since $u_I - \Pi_K u$ is linear on e, and u and u_I match at the end points $\mathbf{a}_e$ and $\mathbf{b}_e$ of e, we obtain

$$\text{(I)} = \left|(u_I - \Pi_K^+ u)|_{\mathbf{a}_e}^{\mathbf{b}_e}\right| = \left|(u - \Pi_K^+ u)|_{\mathbf{a}_e}^{\mathbf{b}_e}\right| = \left|\int_e \partial_e(u - \Pi_K^+ u)\,\mathrm{d}s\right| \le h_e^{1/2}|u - \Pi_K^+ u|_{1,e}. \tag{5.24}$$

Replacing u by its extension u_E^+ and recalling that $\Pi_K^+ u$ is a polynomial being trivially used on the whole element K, we apply the standard trace inequality and Lemma 13 to get

$$\text{(I)} \le h_K^{1/2}|u_E^+ - \Pi_K^+ u|_{1,\hat{e}} \lesssim |u_E^+ - \Pi_K^+ u|_{1,K} + h_K|u_E^+|_{2,K} \lesssim h_K\|u_E^{\pm}\|_{2,\omega_K} + |u_E^{\pm}|_{1,\delta K}. \tag{5.25}$$

For (II), applying the trace inequality for IFE functions in Theorem 11, and Lemma 21, we obtain

$$\begin{aligned}\text{(II)} = \left|\Pi_K(u - u_I)|_{\mathbf{a}_e}^{\mathbf{b}_e}\right| &= \left|\int_e \partial_e\Pi_K(u - u_I)\,\mathrm{d}s\right|\\ \le h_e^{1/2}|\Pi_K(u - u_I)|_{1,\hat{e}} &\lesssim h_K^{-1/2}h_e^{1/2}|\Pi_K(u - u_I)|_{1,K} \le h_K\|u_E^{\pm}\|_{2,\omega_K}.\end{aligned} \tag{5.26}$$

Combining the estimates of (I) and (II), we have the desired result. □

Combining the results of Lemmas 21, 22 and 23 and the error bound in Theorem 5.1, we achieve the following conclusion.

Theorem 5.2 *Let $u \in H^2(\beta; \mathcal{T}_h)$ be the solution to (1.1) and u_h be the solution to (5.5), we have*

$$|||u - u_h|||_n \lesssim h\|u\|_{2,\cup\Omega^{\pm}}. \tag{5.27}$$

Proof The triangle inequality yields $|||u-u_h|||_n \le |||u-u_I|||_n + |||u_I-u_h|||_n$. For $|||u_I-u_h|||_n$, combining the results of Lemmas 21, 22 and 23 and the error bound in Theorem 5.1, we have

$$\begin{aligned} |||u_I-u_h|||_n &\lesssim \sum_{K\in\mathcal{T}_h^n} h_K\|u\|_{2,K} + \sum_{K\in\mathcal{T}_h^i}\left(h_K\|u\|_{E,2,\omega_K} + |u|_{E,1,\delta K}\right) \\ &\lesssim h\|u\|_{E,2,\Omega} \lesssim h\|u\|_{2,\cup\Omega^\pm}, \end{aligned} \tag{5.28}$$

where we have used the finite overlapping property of ω_K and the strip argument in Lemma 2 to control $|u|_{1,\delta K}$ and finally the boundedness for Sobolev extensions.

Then we proceed to estimate $|||u-u_I|||_n$. Since it is trivial on non-interface elements, we only need to estimate it on interface elements. By the triangle inequality, we have

$$|||u-u_I|||_n \lesssim \sum_{K\in\mathcal{T}_h^i}\left(\|\beta_h^{1/2}\nabla\Pi_K(u-u_I)\|_{0,K} + |u-u_I|_{1/2,\mathcal{E}_K}\right) + \sum_{K\in\mathcal{T}_h^n} h_K\|u\|_{2,K}. \tag{5.29}$$

The first term can be handled by Lemma 21. For the second term, given $e\in\mathcal{E}_K$ and without loss of generality assuming it is K_h^+, by the interpolation estimate in 1D and the trace inequality [10, Lemma 6.2], we have

$$|u-u_I|_{1/2,e} \lesssim h_e|u|_{3/2,e} \lesssim h_e|u_E^+|_{3/2,\hat{e}} \lesssim h_K\|u_E^+\|_{2,K} \tag{5.30}$$

where $\hat{e}$ is the extension of e. Putting (5.30) to (5.29) and applying the boundedness for Sobolev extensions, we have the desired result. □

6 H(curl) Interface Problems

In this section, we present an IVEM for the $\mathbf{H}(\mathrm{curl})$-elliptic interface problem and give an optimal order error estimate.

6.1 Scheme

We first present the scheme for the $\mathbf{H}(\mathrm{curl})$ interface problem. Define the local discrete bilinear form on an interface element K as: $a_h^{e,K}(\cdot,\cdot) : \mathbf{H}(\mathrm{curl};K)\times\mathbf{H}(\mathrm{curl};K)\to\mathbb{R}$ where

$$\begin{aligned} a_h^{e,K}(\mathbf{u}_h,\mathbf{v}_h) := {} & (\alpha_h\,\mathrm{curl}\,\mathbf{u}_h,\mathrm{curl}\,\mathbf{v}_h)_K + (\beta_h\boldsymbol{\Pi}_K\mathbf{u}_h,\boldsymbol{\Pi}_K\mathbf{v}_h)_K \\ & + S_K^e(\mathbf{u}_h-\boldsymbol{\Pi}_K\mathbf{u}_h,\mathbf{v}_h-\boldsymbol{\Pi}_K\mathbf{v}_h). \end{aligned} \tag{6.1}$$

Similarly, $\boldsymbol{\Pi}_K$ reduces to an identity operator on non-interface elements, and thus the local bilinear forms do not contain any projection or stabilization terms. Following [12], using the same β_e in (5.4), we directly employ the DoFs to construct the stabilization $S_K^e(\cdot,\cdot)$:

$$S_K^e(\mathbf{w}_h,\mathbf{z}_h) := \sum_{e\in\mathcal{E}_K}\beta_e(\mathbf{w}_h\cdot\mathbf{t},\mathbf{z}_h\cdot\mathbf{t})_{0,e}. \tag{6.2}$$

With these preparations, the IVEM for solving (1.3a) is to find $\mathbf{u}_h\in\mathbf{V}_h^e$ such that

$$a_h^e(\mathbf{u}_h,\mathbf{v}_h) := \sum_{K\in\mathcal{T}_h} a_h^{e,K}(\mathbf{u}_h,\mathbf{v}_h) = \sum_{K\in\mathcal{T}_h}(\mathbf{f},\boldsymbol{\Pi}_K\mathbf{v}_h)_K, \quad \forall\mathbf{v}_h\in\mathbf{V}_h^e, \tag{6.3}$$

where the local bilinear form on non-interface elements is the standard one $(\alpha_h \operatorname{curl} \mathbf{u}_h, \operatorname{curl} \mathbf{v}_h) + (\beta_h \mathbf{u}_h, \mathbf{v}_h)$.

Remark 6 Note that the scaling in (6.2) is different from the conventional VEM using h [12, 67, 70] (or $h^{1/2}$ on the boundary terms in the induced norm). In this work, the proposed stabilization term above is larger than the one with the h weight, yet this will not downgrade the coercivity constant to become mesh size dependent, see Lemma 25 below. The consistency error may consequently become bigger. However, since the stabilization is only needed near the interface, the overall consistency error is still of the optimal order. We postpone the detailed mathematical reasoning to Remark 8. Here we emphasize that the constant weight stabilization is one of the keys to ensure the optimal order of convergence, see Lemma 30 and Remark 8.

6.2 Coercivity

We begin with defining an energy norm:

$$|||\mathbf{v}_h|||_e^2 := a_h^e(\mathbf{v}_h, \mathbf{v}_h). \tag{6.4}$$

We first show the quantity in (6.4) is indeed a norm.

Lemma 24 *Given $\mathbf{v}_h \in \mathbf{V}_h^e(K)$, there holds*

$$\|\mathbf{v}_h\|_{0,K} \lesssim \frac{\beta_{\max}}{\beta_{\min}} \left(h_K \|\operatorname{curl} \mathbf{v}_h\|_{0,K} + h_K^{1/2} \sum_{e \in \mathcal{E}_K} \|\mathbf{v}_h \cdot \mathbf{t}\|_{0,e} \right). \tag{6.5}$$

Proof Given each $\mathbf{v}_h \in \mathbf{V}_h^e(K)$, let φ_h be the corresponding function in Remark 5. Then, $-\nabla \cdot (\beta_h^{-1} \nabla \varphi) = \operatorname{curl} \mathbf{v}_h$ and $\beta_h^{-1} \nabla \varphi \cdot \mathbf{n} = -\mathbf{v}_h \cdot \mathbf{t}$ on ∂K. Using integration by parts, we obtain

$$\begin{aligned} \|\mathbf{v}_h\|_{0,K}^2 &= \int_K \beta_h^{-1} \mathbf{curl} \varphi_h \cdot \beta_h^{-1} \mathbf{curl} \varphi_h \, \mathrm{d}\mathbf{x} \lesssim \beta_{\min}^{-1} \int_K \beta_h^{-1} \nabla \varphi_h \cdot \nabla \varphi_h \, \mathrm{d}\mathbf{x} \\ &= \beta_{\min}^{-1} \Big(- \int_K \varphi_h \nabla \cdot (\beta_h^{-1} \nabla \varphi_h) \, \mathrm{d}\mathbf{x} + \int_{\partial K} \varphi_h \beta_h^{-1} \nabla \varphi_h \cdot \mathbf{n} \, \mathrm{d}s \Big) \\ &\lesssim \beta_{\min}^{-1} \Big(\|\varphi_h\|_{0,K} \|\operatorname{curl} \mathbf{v}_h\|_{0,K} + \|\varphi_h\|_{0,\partial K} \|\mathbf{v}_h \cdot \mathbf{t}\|_{0,\partial K} \Big). \end{aligned} \tag{6.6}$$

Applying (3.42) and cancelling one term of $\|\mathbf{v}_h\|_{0,K}$ leads to the desired result. □

We highlight that the hidden constant in Lemma 24 is still independent of the interface location. But, compared with Proposition 4.1 of [70], our result involves the extra term $h_K \|\operatorname{curl} \mathbf{v}_h\|_{0,K}$. It yields the following coercivity.

Lemma 25 *For all $\mathbf{v}_h \in \mathbf{V}_h^e$, there holds*

$$\|\mathbf{v}_h\|_{\mathbf{H}(\operatorname{curl};\Omega)} \lesssim |||\mathbf{v}_h|||_e. \tag{6.7}$$

Proof As the norm induced by $a_h^{e,K}(\cdot,\cdot)$ agrees with $\|\cdot\|_{\mathbf{H}(\operatorname{curl};\Omega)}$ on non-interface elements, it suffices to establish the estimates on an interface element K. The triangle inequality directly yields

$$\|\mathbf{v}_h\|_{0,K} \le \|\mathbf{\Pi}_K \mathbf{v}_h\|_{0,K} + \|\mathbf{v}_h - \mathbf{\Pi}_K \mathbf{v}_h\|_{0,K}. \tag{6.8}$$

We note that $\mathbf{\Pi}_K \mathbf{v}_h \in \mathbf{V}_h^e(K)$, then it follows from Lemma 24 and $h_K \lesssim \mathcal{O}(1)$ that

$$\|\mathbf{v}_h - \mathbf{\Pi}_K \mathbf{v}_h\|_{0,K} \lesssim h_K \|\operatorname{curl} \mathbf{v}_h\|_{0,K} + h_K^{1/2} \sum_{e \in \mathcal{E}_K} \|(\mathbf{v}_h - \mathbf{\Pi}_K \mathbf{v}_h) \cdot \mathbf{t}\|_{0,e}. \tag{6.9}$$

Summing up (6.8) and (6.9) on all elements yields the desired result. □

Remark 7 In particular, (6.7) implies the coercivity of the bilinear form $a_h^{e,K}(\cdot,\cdot)$, and thus guarantees the existence and uniqueness of the solution to (6.3). Comparing (6.9) and the stabilization term (6.2), we see that such coercivity still holds independent of the mesh size as the applied stabilization is stronger ($\mathcal{O}(1)$ v.s. $\mathcal{O}(h_K^{1/2})$).

6.3 An Error Equation

Similar to the H^1 case, the analysis is based on the following error decomposition:

$$\boldsymbol{\xi}_h = \mathbf{u} - \mathbf{u}_I \qquad \text{and} \qquad \boldsymbol{\eta}_h = \mathbf{u}_h - \mathbf{u}_I, \tag{6.10}$$

where $\mathbf{u}_I$ is given by (3.25). Let us present the error equation and error bounds.

Lemma 26 (Error equation) *Let* $\mathbf{u} \in \mathbf{H}^1(\operatorname{curl}, \alpha, \beta; \mathcal{T}_h)$ *be the solution to* (1.3a) *and* $\mathbf{u}_h$ *be the solution to* (6.3). *Then the following identity holds*

$$\begin{aligned} |||\boldsymbol{\eta}_h|||_e^2 = \sum_{K \in \mathcal{T}_h} \Big\{ \int_{\partial K} \alpha_h (\operatorname{curl} \mathbf{u} - \operatorname{curl} \mathbf{u}_I)(\boldsymbol{\eta}_h \cdot \mathbf{t} - \mathbf{\Pi}_K \boldsymbol{\eta}_h \cdot \mathbf{t}) \, \mathrm{d}s + ((\beta - \beta_h)\mathbf{u}, \mathbf{\Pi}_K \boldsymbol{\eta}_h)_K \\ + (\beta_h(\mathbf{u} - \mathbf{\Pi}_K \mathbf{u}_I), \mathbf{\Pi}_K \boldsymbol{\eta}_h)_K - S_K^e(\mathbf{u} - \mathbf{\Pi}_K \mathbf{u}_I, \boldsymbol{\eta}_h - \mathbf{\Pi}_K \boldsymbol{\eta}_h) \Big\}. \end{aligned} \tag{6.11}$$

Proof We proceed similarly as (5.9) in Lemma 20. Using the discretized problem (6.3), the original PDE (1.3a), and integration by parts elementwisely, we have

$$\begin{aligned} |||\boldsymbol{\eta}_h|||_e^2 &= a_h^e(\mathbf{u}_h, \boldsymbol{\eta}_h) - a_h^e(\mathbf{u}_I, \boldsymbol{\eta}_h) \\ &= \sum_{K \in \mathcal{T}_h} (\mathbf{f}, \mathbf{\Pi}_K \boldsymbol{\eta}_h)_K - (\alpha_h \operatorname{curl} \mathbf{u}_I, \operatorname{curl} \boldsymbol{\eta}_h)_K - (\beta_h \mathbf{\Pi}_K \mathbf{u}_I, \mathbf{\Pi}_K \boldsymbol{\eta}_h)_K \\ &\quad - S_K^e(\mathbf{u}_I - \mathbf{\Pi}_K \mathbf{u}_I, \boldsymbol{\eta}_h - \mathbf{\Pi}_K \boldsymbol{\eta}_h) \\ &= \sum_{K \in \mathcal{T}_h} \underbrace{(\mathbf{curl}\, \alpha \operatorname{curl} \mathbf{u}, \mathbf{\Pi}_K \boldsymbol{\eta}_h)_K}_{\text{(Ia)}} - \underbrace{(\alpha_h \operatorname{curl} \mathbf{u}_I, \operatorname{curl} \boldsymbol{\eta}_h)_K}_{\text{(Ib)}} \\ &\quad + \underbrace{(\beta \mathbf{u}, \mathbf{\Pi}_K \boldsymbol{\eta}_h)}_{\text{(IIa)}} - \underbrace{(\beta_h \mathbf{\Pi}_K \mathbf{u}_I, \mathbf{\Pi}_K \boldsymbol{\eta}_h)_K}_{\text{(IIb)}} - S_K^e(\mathbf{u}_I - \mathbf{\Pi}_K \mathbf{u}_I, \boldsymbol{\eta}_h - \mathbf{\Pi}_K \boldsymbol{\eta}_h). \end{aligned} \tag{6.12}$$

For (Ia), integration by parts and the continuity conditions for $\operatorname{curl} \mathbf{u} \in \widetilde{H}^1(\alpha, \mathcal{T}_h)$ and $\boldsymbol{\eta}_h \in \mathbf{H}(\operatorname{curl}; \Omega)$ imply

$$\begin{aligned} \sum_{K \in \mathcal{T}_h} (\text{Ia}) &= - \sum_{K \in \mathcal{T}_h} \int_{\partial K} \alpha \operatorname{curl} \mathbf{u} \, (\mathbf{\Pi}_K \boldsymbol{\eta}_h \cdot \mathbf{t}) \\ &\quad \mathrm{d}s = \sum_{K \in \mathcal{T}_h} \int_{\partial K} \alpha \operatorname{curl} \mathbf{u} \, (\boldsymbol{\eta}_h \cdot \mathbf{t} - \mathbf{\Pi}_K \boldsymbol{\eta}_h \cdot \mathbf{t}) \, \mathrm{d}s. \end{aligned} \tag{6.13}$$

In addition, since α_h curl $\mathbf{u}_I$ is a constant and $\mathbf{\Pi}_K \boldsymbol{\eta}_h \in \nabla S_h^n(K)$ by the exact sequence (3.38), we obtain

$$\int_{\partial K} \alpha_h \operatorname{curl} \mathbf{u}_I \, (\mathbf{\Pi}_K \boldsymbol{\eta}_h \cdot \mathbf{t}) \, \mathrm{d}s = \alpha_h \operatorname{curl} \mathbf{u}_I \int_{\partial K} \mathbf{\Pi}_K \boldsymbol{\eta}_h \cdot \mathbf{t} \, \mathrm{d}s = 0. \tag{6.14}$$

So, using integration by parts again together with (6.14), we have

$$(\mathrm{Ib}) = \int_{\partial K} \alpha_h \operatorname{curl} \mathbf{u}_I (\boldsymbol{\eta}_h \cdot \mathbf{t}) \, \mathrm{d}s = \int_{\partial K} \alpha_h \operatorname{curl} \mathbf{u}_I (\boldsymbol{\eta}_h \cdot \mathbf{t} - \mathbf{\Pi}_K \boldsymbol{\eta}_h \cdot \mathbf{t}) \, \mathrm{d}s. \tag{6.15}$$

As α matches α_h on ∂K, we obtain

$$\sum_{K \in \mathcal{T}_h} (\mathrm{Ia}) + (\mathrm{Ib}) = \sum_{K \in \mathcal{T}_h} \int_{\partial K} \alpha_h (\operatorname{curl} \mathbf{u} - \operatorname{curl} \mathbf{u}_I)(\boldsymbol{\eta}_h \cdot \mathbf{t} - \mathbf{\Pi}_K \boldsymbol{\eta}_h \cdot \mathbf{t}) \, \mathrm{d}s. \tag{6.16}$$

For the terms (II), we simply have

$$(\mathrm{IIa}) - (\mathrm{IIb}) = ((\beta - \beta_h)\mathbf{u}, \mathbf{\Pi}_K \boldsymbol{\eta}_h)_K + (\beta_h(\mathbf{u} - \mathbf{\Pi}_K \mathbf{u}_I), \mathbf{\Pi}_K \boldsymbol{\eta}_h)_K. \tag{6.17}$$

As for the stabilization term, using the fact that $(\boldsymbol{\eta}_h - \mathbf{\Pi}_K \boldsymbol{\eta}_h) \cdot \mathbf{t} =: c$ is a constant on e, applying the definition of the interpolation $\int_e (\mathbf{u}_I \cdot \mathbf{t}) c \, \mathrm{d}s = \int_e (\mathbf{u} \cdot \mathbf{t}) c \, \mathrm{d}s$ yields the desired result. □

With the error equation above, we are able to derive the error bound for $\boldsymbol{\eta}_h$.

Theorem 6.1 (A priori error bound) *Let* $\mathbf{u} \in \mathbf{H}^1(\operatorname{curl}, \alpha, \beta; \mathcal{T}_h)$ *be the solution to* (1.3a) *and* $\mathbf{u}_h$ *be the solution to* (6.3). *Then it follows that*

$$\begin{aligned} |||\boldsymbol{\eta}_h|||_e \lesssim \sum_{K \in \mathcal{T}_h} \Big(& \|\alpha_h (\operatorname{curl} \mathbf{u} - \operatorname{curl} \mathbf{u}_I)\|_{0,\partial K} + \|\sqrt{\beta_h} \, (\mathbf{u} - \mathbf{\Pi}_K \mathbf{u}_I)\|_{0,K} \\ & + \|\sqrt{\beta_h} \, (\mathbf{u} - \mathbf{\Pi}_K \mathbf{u}_I)\|_{0,\partial K} \Big) + h \|\mathbf{u}\|_{1,\Omega}. \end{aligned} \tag{6.18}$$

Proof It directly follows from the Cauchy-Schwarz inequality and the definition of stabilization $S_K^e(\cdot, \cdot)$, where the last term is due to Lemma 2. □

6.4 Convergence Analysis

We proceed to estimate each term in (6.18).

Lemma 27 *Let* $\mathbf{u} \in \mathbf{H}^1(\operatorname{curl}, \alpha, \beta; \mathcal{T}_h)$. *Then it follows that*

$$\|\alpha_h (\operatorname{curl} \mathbf{u} - \operatorname{curl} \mathbf{u}_I)\|_{0,\partial K} \lesssim h_K^{1/2} \|\mathbf{u}\|_{E,\operatorname{curl},1,\omega_K}. \tag{6.19}$$

Proof Since K is shape regular, given an edge $e \in \mathcal{E}_K$, suppose $e \subset \partial K^+$ without loss of generality, then applying the trace inequality in Lemma 3 for extensions on the whole K yields

$$\|\operatorname{curl} \mathbf{u} - \operatorname{curl} \mathbf{u}_I\|_{0,e} \lesssim h_K^{-1/2} \|\operatorname{curl} \mathbf{u}_E^+ - \operatorname{curl} \mathbf{u}_I^+\|_{0,K} + h_K^{1/2} |\operatorname{curl} \mathbf{u}_E^+|_{1,K} \tag{6.20}$$

which yields the desired result by (4.18b) in Lemma 17. □

In order to estimate the rest terms of (6.18), we need the following result.

Lemma 28 *Let* $\mathbf{u} \in \mathbf{H}^1(\text{curl}, \alpha, \beta; \mathcal{T}_h)$. *Then it follows that*

$$\|\sqrt{\beta_h}\,\mathbf{\Pi}_K(\mathbf{u}-\mathbf{u}_I)\|_{0,K} \lesssim h_K\|\mathbf{u}\|_{E,1,K}. \tag{6.21}$$

Proof Since $\mathbf{\Pi}_K(\mathbf{u}-\mathbf{u}_I) \in \nabla S_h(K)$, by (3.41) we have a $\varphi_h \in \widetilde{S}_h^n(K)$ from Remark 5 such that $\mathbf{curl}\,\varphi_h = \beta_h\mathbf{\Pi}_K(\mathbf{u}-\mathbf{u}_I)$. Then, integration by parts leads to

$$\|\sqrt{\beta_h}\,\mathbf{\Pi}_K(\mathbf{u}-\mathbf{u}_I)\|_{0,K}^2 = \int_K \mathbf{curl}\,\varphi_h\cdot(\mathbf{u}-\mathbf{u}_I)\,\mathrm{d}\mathbf{x} = -\int_{\partial K}\varphi_h(\mathbf{u}-\mathbf{u}_I)\cdot\mathbf{t}\,\mathrm{d}s. \tag{6.22}$$

Next, the Hölder's inequality, estimate (3.42), and the definition of $\mathbf{u}_I$ together lead to

$$\begin{aligned}\|\sqrt{\beta_h}\,\mathbf{\Pi}_K(\mathbf{u}-\mathbf{u}_I)\|_{0,K}^2 &\le \|\varphi_h\|_{0,\partial K}\|(\mathbf{u}-\mathbf{u}_I)\cdot\mathbf{t}\|_{0,\partial K}\\ &\lesssim h_K^{1/2}\|\beta_h\mathbf{\Pi}_K(\mathbf{u}-\mathbf{u}_I)\|_{0,K}\,h_K^{1/2}\|\mathbf{u}\|_{1/2,\partial K}.\end{aligned} \tag{6.23}$$

Note that $\|\mathbf{u}\|_{1/2,\partial K} \lesssim \|\mathbf{u}\|_{E,1,K}$. Hence, cancelling one term $\|\sqrt{\beta_h}\,\mathbf{\Pi}_K(\mathbf{u}-\mathbf{u}_I)\|_{0,K}$ yields the desired result. □

Lemma 29 *Let* $\mathbf{u} \in \mathbf{H}^1(\text{curl}, \alpha, \beta; \mathcal{T}_h)$. *Then it follows that*

$$\|\sqrt{\beta_h}\,(\mathbf{u}-\mathbf{\Pi}_K\mathbf{u}_I)\|_{0,K} \lesssim h_K\|\mathbf{u}\|_{E,\text{curl},1,\omega_K} + \|\mathbf{u}\|_{E,0,\delta K}. \tag{6.24}$$

Proof The desired result directly follows from the following decomposition

$$\|\sqrt{\beta_h}\,(\mathbf{u}-\mathbf{\Pi}_K\mathbf{u}_I)\|_{0,K} \le \|\sqrt{\beta_h}\,(\mathbf{u}-\mathbf{\Pi}_K\mathbf{u})\|_{0,K} + \|\sqrt{\beta_h}\,\mathbf{\Pi}_K(\mathbf{u}-\mathbf{u}_I)\|_{0,K} \tag{6.25}$$

together with (4.19) and Lemma 28. □

Lemma 30 *Let* $\mathbf{u} \in \mathbf{H}^1(\text{curl}, \alpha, \beta; \mathcal{T}_h)$. *Then it follows that*

$$\|\sqrt{\beta_h}(\mathbf{u}-\mathbf{\Pi}_K\mathbf{u}_I)\|_{0,\partial K} \lesssim h_K^{1/2}\|\mathbf{u}\|_{E,\text{curl},1,\omega_K}. \tag{6.26}$$

Proof Similar to (6.25), we first write

$$\|\sqrt{\beta_h}\,(\mathbf{u}-\mathbf{\Pi}_K\mathbf{u}_I)\|_{0,\partial K} \le \|\sqrt{\beta_h}\,(\mathbf{u}-\mathbf{\Pi}_K\mathbf{u})\|_{0,\partial K} + \|\sqrt{\beta_h}\,\mathbf{\Pi}_K(\mathbf{u}-\mathbf{u}_I)\|_{0,\partial K}. \tag{6.27}$$

Then, using a similar trace inequality argument with that in Lemma 27 and (4.18a) in Lemma 17 lead to

$$\|\mathbf{u}-\mathbf{\Pi}_K\mathbf{u}\|_{0,e} \lesssim h_K^{-1/2}\|\mathbf{u}_E^+ - \mathbf{\Pi}_K^+\mathbf{u}\|_{0,K} + h_K^{1/2}|\mathbf{u}_E^+|_{1,K} \lesssim h_K^{1/2}\|\mathbf{u}\|_{E,\text{curl},1,\omega_K}. \tag{6.28}$$

The estimate of the second term in (6.27) follows from the trace inequality for IFE functions in Lemmas 18 and 28. □

We are ready to present the main theorem in this section.

Theorem 6.2 *Let* $\mathbf{u} \in \mathbf{H}^1(\text{curl}, \alpha, \beta; \mathcal{T}_h)$ *be the solution to (1.3a) and* $\mathbf{u}_h$ *be the solution to (6.3). Then,*

$$|||\mathbf{u}-\mathbf{u}_h|||_e \lesssim h_K\|\mathbf{u}\|_{\mathbf{H}^1(\text{curl};\cup\Omega^\pm)}. \tag{6.29}$$

Proof Note the decomposition $\mathbf{u}-\mathbf{u}_h = \boldsymbol{\xi}_h + \boldsymbol{\eta}_h$ in (6.10). The estimates on non-interface elements are standard. Using Theorem 6.1 with the Lemmas 27–30, we obtain

$$\begin{aligned}|||\boldsymbol{\eta}_h|||_e &\lesssim \sum_{K\in\mathcal{T}_h^i}\left(h_K^{1/2}\|\mathbf{u}\|_{E,\text{curl},1,\omega_K} + \|\mathbf{u}\|_{E,0,\delta K}\right) + \sum_{K\in\mathcal{T}_h^n} h_K\|\mathbf{u}\|_{\mathbf{H}^1(\text{curl};K)}\\ &\lesssim h_K^{1/2}\|\mathbf{u}\|_{E,\text{curl},1,\Omega_{h_\Gamma}} + \|\mathbf{u}\|_{E,\text{curl},1,\Omega_{\delta_0}} + h\|\mathbf{u}\|_{\mathbf{H}^1(\text{curl};\cup\Omega^\pm)} \lesssim h\|\mathbf{u}\|_{\mathbf{H}^1(\text{curl};\cup\Omega^\pm)},\end{aligned} \tag{6.30}$$

where we have used Lemma 2 with the estimates for h_Γ and δ_0. In addition, by the definition of $|||\cdot|||_e$, we have

$$|||\boldsymbol{\xi}_h|||_e \lesssim \sum_{K\in\mathcal{T}_h} \|\operatorname{curl}\boldsymbol{\xi}_h\|_{0,K} + \|\boldsymbol{\Pi}_K\boldsymbol{\xi}_h\|_{0,K} + \|\boldsymbol{\xi}_h - \boldsymbol{\Pi}_K\boldsymbol{\xi}_h\|_{0,\partial K} \tag{6.31}$$

where the estimates of the first two terms follow from (4.18b) in Lemma 17 and Lemma 28, respectively. For the last term in (6.31), we notice that

$$\|(\mathbf{u}-\mathbf{u}_I) - \boldsymbol{\Pi}_K(\mathbf{u}-\mathbf{u}_I)\|_{0,\partial K} \le \|\mathbf{u}-\mathbf{u}_I\|_{0,\partial K} + \|\boldsymbol{\Pi}_K(\mathbf{u}-\mathbf{u}_I)\|_{0,\partial K} \tag{6.32}$$

where the estimate of the first term is similar to (6.23), and the estimate of the second term comes from the trace inequality for IFE functions in Theorem 11 together with Lemma 28. □

Remark 8 If the "right" scaling h is used in stabilization (6.2) that induces a discrete $H^{-1/2}$ norm to match the regularity of the trace of an $\mathbf{H}(\text{curl})$ vector field in 2D, then, in the derivation of the a priori error bound in Theorem 6.1, one has to use the following estimate:

$$\begin{aligned}&\int_{\partial K} \alpha_h(\operatorname{curl}\mathbf{u} - \operatorname{curl}\mathbf{u}_I)(\boldsymbol{\eta}_h\cdot\mathbf{t} - \boldsymbol{\Pi}_K\boldsymbol{\eta}_h\cdot\mathbf{t})\,\mathrm{d}s\\ &\quad\le h^{-1/2}\|\alpha_h(\operatorname{curl}\mathbf{u} - \operatorname{curl}\mathbf{u}_I)\|_{0,\partial K} h^{1/2}\|\boldsymbol{\eta}_h\cdot\mathbf{t} - \boldsymbol{\Pi}_K\boldsymbol{\eta}_h\cdot\mathbf{t}\|_{0,\partial K}.\end{aligned} \tag{6.33}$$

Opting for this route, the term $h^{1/2}\|\boldsymbol{\eta}_h\cdot\mathbf{t} - \boldsymbol{\Pi}_K\boldsymbol{\eta}_h\cdot\mathbf{t}\|_{0,\partial K}$ is a part of the norm $|||\boldsymbol{\eta}_h|||_e$. Thus, the term $h^{-1/2}\|\alpha_h(\operatorname{curl}\mathbf{u} - \operatorname{curl}\mathbf{u}_I)\|_{0,\partial K}$ needs to yield an h to deliver the optimal order convergence. However, using (6.19) in Lemma 27 to estimate this term will immediately lead to the loss of a further $h^{1/2}$ order convergence, such that the final error estimate is only suboptimal. Furthermore, we highlight that such a trick to achieve optimal convergence highly relies on the property that VEM can obtain coercivity even for an "underweight" scaling parameter. In contrast, h^{-1} scaling has to be used for the purpose of coercivity (norm equivalence) in some unfitted mesh methods, which causes suboptimal convergence.

7 Numerical Experiments

In this section, we present some numerical results to validate the analysis above. Here we focus on the $\mathbf{H}(\text{curl})$ problem, as the main motivation for this work is to address the related non-conformity issue that challenges many unfitted mesh methods [14, 15, 31]. We consider a domain $\Omega = (-1,1)\times(-1,1)$ with a structured Cartesian triangular mesh. Our test example is borrowed from [34] where the interface is a circle given by $\Gamma: x^2+y^2 = r_1^2$ that cuts Ω into the inside and outside subdomains denoted by Ω^- and Ω^+. The exact solution is given by

$$\mathbf{u} = \begin{cases} \frac{1}{\alpha^-}\begin{pmatrix}(-k_1(r_1^2-x^2-y^2)y)\\ (-k_1(r_1^2-x^2-y^2)x)\end{pmatrix} & \text{in } \Omega^-,\\ \frac{1}{\alpha^+}\begin{pmatrix}(-k_2(r_2^2-x^2-y^2)(r_1^2-x^2-y^2)y)\\ (-k_2(r_2^2-x^2-y^2)(r_1^2-x^2-y^2)x)\end{pmatrix} & \text{in } \Omega^+.\end{cases} \tag{7.1}$$

The boundary conditions and the right hand side $\mathbf{f}$ are calculated accordingly. We set $k_2 = 20$, $k_1 = k_2(r_2^2 - r_1^2)$ with $r_1 = \pi/5$ and $r_2 = 1$, and consider the parameters: fixing $\alpha^- = \beta^- = 1$ and varying $\alpha^+ = \beta^+ = 10$ or 100. We present the numerical results in the following

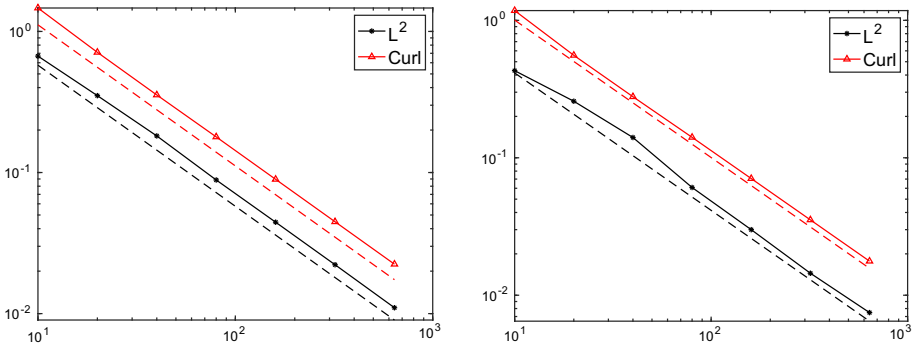

Fig. 4 Errors of the IVE for the $\mathbf{H}(\mathrm{curl})$ interface problem: $\alpha^+ = \beta^+ = 10$ (left) and $\alpha^+ = \beta^+ = 100$ (right). The dashed lines are the reference lines indicating an optimal convergence of order $\mathcal{O}(h)$

Fig. 4 which clearly show an optimal convergence and outperform many other unfitted mesh methods in the literature.

8 Concluding Remarks

We have developed IVE methods for solving H^1 and $\mathbf{H}(\mathrm{curl})$ elliptic interface problems in two dimensions. Conventional finite element spaces are conforming but do not satisfy the jump conditions, while the IFE spaces in current literature satisfy the jump conditions but are not conforming. The proposed IVE spaces are conforming and satisfy the jump conditions simultaneously. In our opinion, they are candidates for the "ideal" spaces to solve interface problems. This unique attribute makes the proposed methods inherit the advantages of both fitted and unfitted mesh methods. Similar to the classic VEM, the newly constructed spaces are projected to the IFE spaces which is computable directly through DoFs.

There are several major differences of the proposed IVEM from the classic IFEM. First, the proposed method does not require those DG-like edge terms originated from integration by parts. The only edge-based term is the stabilization term. Opposing to IPDG-like methods that has the symmetry-coercive dilemma, what is even more favorable about IVEM is that the resulting discretization is parameter-free, and yields a symmetric system which can be solved by fast linear solvers. This is particularly useful for the $\mathbf{H}(\mathrm{curl})$ case, since it avoids using h^{-1} scaling in the stabilization that causes a loss of convergence order for non-conforming methods [14, 15, 31]. Second, the stabilization is completely local, and consequently the assembling does not need to compute the interaction between two neighbor elements' DoFs. This trait makes this method more parallelizable. In addition, there are more DoFs locally on each interface element than classic IFEM, and these extra DoFs are introduced by the cutting points which can better resolve the geometry.

The proposed method is also distinguished from the classic VEM in the fact that anisotropic elements cut by the interface are treated together as a shape regular element. Thanks to this treatment and the properties of IFE spaces, the robust error analysis with respect to cutting points can be achieved which is also much easier and more systematic. In fact, for the analysis of classical VEM on anisotropic elements [10, 12], the main difficulty is to obtain an error bound that is independent of element anisotropy such as shrinking elements. We

highlight that one of the key obstacles for anisotropic analysis is the failure of the standard trace inequalities as the height of an edge may be very small and thus unable to support a smooth extension of a function defined on an edge toward the interior. For example for the present situation, in the estimation of (5.19) and (5.26), the standard trace inequality cannot be applied directly to each polynomial on each subelement as it may shrink, and thus the hidden constant may not be uniform with respect h anymore. Consequently, the estimation for VEM generally requires some dedicated analysis techniques such as the Poincaré inequality on an anisotropic cut element developed in [10, 12]. This is especially difficult for the $\mathbf{H}(\text{curl})$ case that demands a virtual mesh, see [12]. These specialized analysis may limit the scope of its applicable elements. However, in the proposed analysis of this paper, these special treatments are not needed anymore. This improvement comes from the benefit of adopting the piecewise polynomial IFE functions as our projection space, which do admit cutting geometry-independent trace inequalities on interface elements as shown in Lemmas 11 and 18. These trace inequalities significantly simplify the analysis, which are now streamlined to resemble more to the standard analysis on isotropic elements.

Similar to many unfitted mesh methods in the literature, the present analysis relies on that the interface is smooth. If the interface is non-smooth (even piecewise smooth), many critical tools for the analysis will not be available anymore. For example, if the interface has geometrical singularities, the solutions will have lower regularity ([59]). Consequently, (i) H^2 and $\mathbf{H}^1(\text{curl})$ Sobolev extensions become obscure, (ii) commuting diagrams with extra smoothness in Sect. 2.2 do not hold anymore.

We focus on two-dimensional problems in this work to introduce the methodology, which can shed light on the 3D case. In a more recent work [13], the IVE spaces and the schemes are extended to the 3D case. As one can imagine, the definition of IVE and IFE spaces as well as anisotropic error analysis in 3D will be much more complicated.

Acknowledgements The authors are grateful for the constructive advice from the anonymous reviewers.

Funding The authors are supported in part by DMS-1913080 and DMS-2012465.

Data Availability Enquiries about data availability should be directed to the authors.

Declarations

Competing Interests The authors have not disclosed any competing interests.

References

1. Adams, R.A., Fournier, J.J.: Sobolev spaces, vol. 140. Elsevier (2003)
2. Anand, A., Ovall, J.S., Reynolds, S.E., Weißer, S.: Trefftz finite elements on curvilinear polygons. SIAM J. Sci. Comput. **42**(2), A1289–A1316 (2020)
3. Arnold, D.N., Falk, R.S., Winther, R.: Finite element exterior calculus: from Hodge theory to numerical stability. Bull. Amer. Math. Soc. **47**, 281–354 (2000)
4. Babuška, I., Aziz, A.K.: On the angle condition in the finite element method. SIAM J. Numer. Anal. **13**(2), 214–226 (1976). https://doi.org/10.1137/0713021
5. Babuška, I., Caloz, G., Osborn, J.E.: Special finite element methods for a class of second order elliptic problems with rough coefficients. SIAM J. Numer. Anal. **31**(4), 945–981 (1994). https://doi.org/10.1137/0731051
6. Babuška, I., Osborn, J.E.: Generalized finite element methods: their performance and their relation to mixed methods. SIAM J. Numer. Anal. **20**(3), 510–536 (1983). https://doi.org/10.1137/0720034

7. Ben Belgacem, F., Buffa, A., Maday, Y.: The mortar finite element method for 3D Maxwell equations: First results. SIAM J. Numer. Anal. **39**(3), 880–901 (2001). https://doi.org/10.1137/S0036142999357968
8. Brenner, S.C., Sung, L.Y.: Virtual element methods on meshes with small edges or faces. Math. Models Methods Appl. Sci. **28**(7), 1291–1336 (2018)
9. Burman, E., Claus, S., Hansbo, P., Larson, M.G., Massing, A.: CutFEM: Discretizing geometry and partial differential equations. Internat. J. Numer. Methods Engrg. **104**(7), 472–501 (2015)
10. Cao, S., Chen, L.: Anisotropic error estimates of the linear virtual element method on polygonal meshes. SIAM J. Numer. Anal. **56**(5), 2913–2939 (2018). https://doi.org/10.1137/17M1154369
11. Cao, S., Chen, L.: Anisotropic error estimates of the linear nonconforming virtual element methods. SIAM J. Numer. Anal. **57**(3), 1058–1081 (2019)
12. Cao, S., Chen, L., Guo, R.: A virtual finite element method for two dimensional Maxwell interface problems with a background unfitted mesh. Math. Models Methods Appl. Sci. **31**(14), 2907–2936 (2021)
13. Cao, S., Chen, L., Guo, R.: Immersed virtual element methods for Maxwell interface problems in three dimensions. arXiv preprint arXiv:2202.09987 (2022)
14. Casagrande, R., Hiptmair, R., Ostrowski, J.: An a priori error estimate for interior penalty discretizations of the Curl-Curl operator on non-conforming meshes. J. Math. Ind. **6**(1), 4 (2016). https://doi.org/10.1186/s13362-016-0021-9
15. Casagrande, R., Winkelmann, C., Hiptmair, R., Ostrowski, J.: Dg treatment of non-conforming interfaces in 3d curl-curl problems. In: Scientific Computing in Electrical Engineering, pp. 53–61. Springer International Publishing, Cham (2016)
16. Chen, L., Huang, J.: Some error analysis on virtual element methods. Calcolo **55**(1), 5 (2018)
17. Chen, L., Huang, X.: Discrete Hessian complexes in three dimensions. arXiv preprint arXiv:2012.10914 (2020)
18. Chen, L., Wei, H., Wen, M.: An interface-fitted mesh generator and virtual element methods for elliptic interface problems. J. Comput. Phys. **334**, 327–348 (2017)
19. Chen, Z., Wu, Z., Xiao, Y.: An adaptive immersed finite element method with arbitrary Lagrangian-Eulerian scheme for parabolic equations in time variable domains. Int. J. Numer. Anal. Model. **12**(3), 567–591 (2015)
20. Chen, Z., Xiao, Y., Zhang, L.: The adaptive immersed interface finite element method for elliptic and Maxwell interface problems. J. Comput. Phys. **228**(14), 5000–5019 (2009). https://doi.org/10.1016/j.jcp.2009.03.044
21. Chen, Z., Zou, J.: Finite element methods and their convergence for elliptic and parabolic interface problems. Numer. Math. **79**(2), 175–202 (1998)
22. Chen, Z., Zou, J.: An augmented Lagrangian method for identifying discontinuous parameters in elliptic systems. SIAM J. Control. Optim. **37**(3), 892–910 (1999)
23. Chu, C.C., Graham, I.G., Hou, T.Y.: A new multiscale finite element method for high-contrast elliptic interface problems. Math. Comp. **79**(272), 1915–1955 (2010). https://doi.org/10.1090/S0025-5718-2010-02372-5
24. Costabel, M., Dauge, M., Nicaise, S.: Singularities of Maxwell interface problems. ESAIM: M2AN **33**(3), 627–649 (1999)
25. Costabel, M., Dauge, M., Nicaise, S.: Corner Singularities of Maxwell Interface and Eddy Current Problems, pp. 241–256. Birkhäuser Basel, Basel (2004). https://doi.org/10.1007/978-3-0348-7926-2_28
26. Edelsbrunner, H.: Triangulations and meshes in computational geometry. Acta Numer **9**, 133–213 (2000)
27. Ern, A., Guermond, J.L.: Finite element quasi-interpolation and best approximation. ESAIM Math. Model. Numer. Anal. **51**(4), 1367–1385 (2017)
28. Guo, R., Lin, T.: A group of immersed finite-element spaces for elliptic interface problems. IMA J. Numer. Anal. **39**(1), 482–511 (2019)
29. Guo, R., Lin, T., Lin, Y.: Approximation capabilities of the immersed finite element spaces for elasticity interface problems. Numer. Methods Partial Differential Equations **35**(3), 1243–1268 (2018). https://doi.org/10.1002/num.22348
30. Guo, R., Lin, T., Zhuang, Q.: Improved error estimation for the partially penalized immersed finite element methods for elliptic interface problems. Int. J. Numer. Anal. Model. **16**(4), 575–589 (2019)
31. Guo, R., Lin, Y., Zou, J.: Solving two dimensional $H(\mathbf{curl})$-elliptic interface systems with optimal convergence on unfitted meshes. arXiv:2011.11905 (2020)
32. Guzmán, J., Sánchez, M.A., Sarkis, M.: A finite element method for high-contrast interface problems with error estimates independent of contrast. J. Sci. Comput. **73**(1), 330–365 (2017)
33. Hansbo, A., Hansbo, P.: An unfitted finite element method, based on Nitsche's method, for elliptic interface problems. Comput. Methods Appl. Mech. Engrg. **191**(47–48), 5537–5552 (2002). https://doi.org/10.1016/S0045-7825(02)00524-8

34. Hiptmair, R., Li, J., Zou, J.: Convergence analysis of finite element methods for H(curl; Ω)-elliptic interface problems. Numer. Math. **122**(3), 557–578 (2012). https://doi.org/10.1007/s00211-012-0468-6
35. Houston, P., Perugia, I., Schneebeli, A., Schötzau, D.: Interior penalty method for the indefinite time-harmonic Maxwell equations. Numer. Math. **100**(3), 485–518 (2005). https://doi.org/10.1007/s00211-005-0604-7
36. Houston, P., Perugia, I., Schötzau, D.: Mixed discontinuous Galerkin approximation of the Maxwell operator. SIAM J. Numer. Anal. **42**(1), 434–459 (2004). https://doi.org/10.1137/S003614290241790X
37. Houston, P., Perugia, I., Schötzau, D.: Mixed discontinuous Galerkin approximation of the Maxwell operator: Non-stabilized formulation. J. Sci. Comput. **22**(1), 315–346 (2005). https://doi.org/10.1007/s10915-004-4142-8
38. Hu, Q., Shu, S., Zou, J.: A mortar edge element method with nearly optimal convergence for three-dimensional Maxwell's equations. Math. Comp. **77**, 1333–1353 (2008)
39. Huang, J., Zou, J.: Some new a priori estimates for second-order elliptic and parabolic interface problems. J. Differential Equations **184**(2), 570–586 (2002). https://doi.org/10.1006/jdeq.2001.4154
40. Huang, J., Zou, J.: Uniform a priori estimates for elliptic and static Maxwell interface problems. Disc. Cont. Dynam. Sys., Series B **7**(1), 145 (2007)
41. Ihlenburg, F., Babuška, I.: Dispersion analysis and error estimation of Galerkin finite element methods for the Helmholtz equation. Int. J. Numer. Meth. Eng. **38**(22), 3745–3774 (1995)
42. Ji, H.: An immersed Raviart-Thomas mixed finite element method for elliptic interface problems on unfitted meshes. J. Sci. Comput. **91**(2), 66 (2022)
43. Ji, H., Wang, F., Chen, J., Li, Z.: Analysis of nonconforming IFE methods and a new scheme for elliptic interface problems. arXiv:2108.03179v2 (2021)
44. Ji, H., Wang, F., Chen, J., Li, Z.: A new parameter free partially penalized immersed finite element and the optimal convergence analysis. Numer. Math. **150**, 1035–1086 (2022)
45. Jirousek, J., Wroblewski, A.: T-elements: state of the art and future trends. Archives of Computational Methods in Engineering **3**(4), 323–434 (1996)
46. Kobayashi, K., Tsuchiya, T.: Error analysis of Lagrange interpolation on tetrahedrons. J. Approx. Theory **249**, 105302 (2020). https://doi.org/10.1016/j.jat.2019.105302
47. Kŕížek, M.: On the maximum angle condition for linear tetrahedral elements. SIAM J. Numer. Anal. **29**(2), 513–520 (1992). https://doi.org/10.1137/0729031
48. LeVeque, R.J., Li, Z.: The immersed interface method for elliptic equations with discontinuous coefficients and singular sources. SIAM J. Numer. Anal. **31**(4), 1019–1044 (1994). https://doi.org/10.1137/0731054
49. Li, J., Melenk, J.M., Wohlmuth, B., Zou, J.: Optimal a priori estimates for higher order finite elements for elliptic interface problems. Appl. Numer. Math. **60**(1), 19–37 (2010)
50. Li, X.Y., Teng, S.H.: Generating well-shaped delaunay meshed in 3d. In: SODA, vol. 1, pp. 28–37 (2001)
51. Li, Z.: The immersed interface method using a finite element formulation. Appl. Numer. Math. **27**(3), 253–267 (1998). https://doi.org/10.1016/S0168-9274(98)00015-4
52. Li, Z., Lin, T., Lin, Y., Rogers, R.C.: An immersed finite element space and its approximation capability. Numer. Methods Partial Differential Equations **20**(3), 338–367 (2004)
53. Lin, T., Lin, Y., Zhang, X.: Partially penalized immersed finite element methods for elliptic interface problems. SIAM J. Numer. Anal. **53**(2), 1121–1144 (2015). https://doi.org/10.1137/130912700
54. Liu, H., Zhang, L., Zhang, X., Zheng, W.: Interface-penalty finite element methods for interface problems in H^1, H(curl), and H(div). Comput. Methods Appl. Mech. Engrg. **367**, 113137 (2020). https://doi.org/10.1016/j.cma.2020.113137
55. Löhner, R., Cebral, J.R., Camelli, F.E., Appanaboyina, S., Baum, J.D., Mestreau, E.L., Soto, O.A.: Adaptive embedded and immersed unstructured grid techniques. Comput. Methods Appl. Mech. Engrg. **197**(25), 2173–2197 (2008). https://doi.org/10.1016/j.cma.2007.09.010
56. Monk, P.: Finite Element Methods for Maxwell's Equations. Oxford University Press (2003)
57. Moore, R., Saigal, S.: Eliminating slivers in three-dimensional finite element models. Laser Phys. **15**(3), 283–291 (2005)
58. Nédélec, J.C.: Mixed finite elements in R^3. Numer. Math. **35**(3), 315–341 (1980). https://doi.org/10.1007/BF01396415
59. Nicaise, S.: Polygonal interface problems: higher regularity results. Comm. Partial Differential Equations **15**(10), 1475–1508 (1990)
60. Nitsche, J.: Über ein Variationsprinzip zur Lösung von Dirichlet-Problemen bei Verwendung von Teilräumen, die keinen Randbedingungen unterworfen sind. Abh. Math. Semin. Univ. Hambg. **36**(1), 9–15 (1971). https://doi.org/10.1007/BF02995904
61. Raviart, P.A., Thomas, J.M.: A mixed finite element method for 2nd order elliptic problems. In: Mathematical aspects of finite element methods (Proc. Conf., Consiglio Naz. delle Ricerche (C.N.R.), Rome, 1975), pp. 292–315. Lecture Notes in Math., Vol. 606. Springer, Berlin (1977)

62. Schöberl, J.: Commuting quasi-interpolation operators for mixed finite elements. 2nd European Conference on Computational Mechanics (2001)
63. Beirão da Veiga, L., Brezzi, F., Cangiani, A., Manzini, G., Marini, L.D., Russo, A.: Basic principles of virtual element methods. Math. Models Methods Appl. Sci. **23**(01), 199–214 (2013). https://doi.org/10.1142/S0218202512500492
64. Beirão da Veiga, L., Brezzi, F., Dassi, F., Marini, L.D., Russo, A.: A family of three-dimensional virtual elements with applications to magnetostatics. SIAM J. Numer. Anal. **56**(5), 2940–2962 (2018). https://doi.org/10.1137/18M1169886
65. Beirão da Veiga, L., Brezzi, F., Marini, L.D., Russo, A.: The hitchhiker's guide to the virtual element method. Math. Models Methods Appl. Sci. **24**(08), 1541–1573 (2014). https://doi.org/10.1142/S021820251440003X
66. Beirão da Veiga, L., Brezzi, F., Marini, L.D., Russo, A.: H(div) and H(curl)-conforming virtual element methods. Numer. Math. **133**(2), 303–332 (2016). https://doi.org/10.1007/s00211-015-0746-1
67. Beirão da Veiga, L., Dassi, F., Manzini, G., Mascotto, L.: Virtual elements for Maxwell's equations. Comput. Math. Appl. **116**, 82–99 (2021)
68. Beirão da Veiga, L., Lovadina, C., Russo, A.: Stability analysis for the virtual element method. Math. Models Methods Appl. Sci. **27**(13), 2557–2594 (2017)
69. Beirão da Veiga, L., Russo, A., Vacca, G.: The virtual element method with curved edges. ESAIM: Mathematical Modelling and Numerical Analysis **53**(2), 375–404 (2019)
70. da Veiga, L.B., Mascotto, L.: Interpolation and stability properties of low order face and edge virtual element spaces. IMA J. Numer. Anal. (2022). https://doi.org/10.1093/imanum/drac008
71. Wang, F., Xiao, Y., Xu, J.: High-order extended finite element methods for solving interface problems. Comput. Methods Appl. Mech. Engrg. **364**(1), 112964 (2020)
72. Wei, H., Chen, L., Huang, Y., Zheng, B.: Adaptive mesh refinement and superconvergence for two-dimensional interface problems. SIAM J. Sci. Comput. **36**(4), A1478–A1499 (2014)
73. Wriggers, P., Rust, W., Reddy, B.: A virtual element method for contact. Comput. Mech. **58**(6), 1039–1050 (2016)
74. Xu, J.: Estimate of the convergence rate of finite element solutions to elliptic equations of second order with discontinuous coefficients. Natur. Sci. J. Xiangtan Univ. **1**(1), 1–5 (1982)
75. Yu, S., Zhou, Y., Wei, G.: Matched interface and boundary (MIB) method for elliptic problems with sharp-edged interfaces. J. Comput. Phys. **224**(2), 729–756 (2007). https://doi.org/10.1016/j.jcp.2006.10.030
76. Zheng, X., Lowengrub, J.: An interface-fitted adaptive mesh method for elliptic problems and its application in free interface problems with surface tension. Adv. Comput. Math. **42**(5), 1225–1257 (2016). https://doi.org/10.1007/s10444-016-9460-5

Publisher's Note Springer Nature remains neutral with regard to jurisdictional claims in published maps and institutional affiliations.

Springer Nature or its licensor holds exclusive rights to this article under a publishing agreement with the author(s) or other rightsholder(s); author self-archiving of the accepted manuscript version of this article is solely governed by the terms of such publishing agreement and applicable law.